

Design of Ultra-Wideband Optical Frequency Comb and Its Implementation in Coherent WDM Systems

Teba Th. Aladwan^[1] and Raad Sami Fyath^[2]

^[1] Department of Laser and Optoelectronics Engineering, AL-Nahrain University

^[2] Department of Computer Engineering, Al-Nahrain University, Baghdad, Iraq

Abstract:

Conventional wavelength-division multiplexing (WDM) systems use a bank of semiconductor lasers at the transmitter side to carry channels data and may use a similar bank at the receiver side to demodulate the data coherently. The power and frequency spacing of the laser's bank should be controlled carefully leading to an increase in the cost and reducing the robustness of the WDM transmitter and receiver. To solve these limitations, an optical frequency comb generator (OFCG) has been proposed in this research to replace the laser banks in WDM systems. This work faces the challenge of how to design an ultra-wideband (UWB) comb with small size and easy frequency tunability to satisfy the requirements of advanced high-bit rate based-WDM systems. This challenge is addressed in this paper. Firstly, the design of an electrooptic modulator (EOM)-based UWB comb is presented. The comb consists of two parallel single-drive push-pull Mach-Zehnder modulators (MZMs) cascaded with an electroabsorption modulator (EAM) and can offer 25, 31, and 39 optical lines with 0.5-, 1, and 3 dB-flatness spectra, respectively. The line frequency spacing Δf of 50, 100, and 150 GHz are reported without affecting the number of generated comb lines. Three of the designed combs are used to generate a 72-line comb of 100 GHz frequency spacing to support an extended C-band WDM system. Then the proposed comb configurations are used in dual-polarization (DP) 16-QAM coherent WDM systems to replaces the laser bank at both the transmitter and receiver sides. The transmission performance of the designed WDM systems is simulated using Optisystem software ver.15. Simulation results are recorded for different values of symbol rate R_s (40, 80, and 120 GSps) which correspond to 0.8 Δf , and for a different number of multiplexed channels (8, 16, 32, and 72). The simulation results indicate that the 32- and 72-channel comb-based WDM system can carry a data rate of 30 and 46 Tbps when the comb is designed with $\Delta f=100$ and 150 GHz, respectively.

I. INTRODUCTION

Recently, there is a rapidly increasing data traffic demand to support advanced applications such as internet-of-things (IoT), wireless, mobile services, and three-dimensional (3D) video streaming [1,2]. Recent developments in optical fiber communication systems and networks open the way to deal with ultra-high data transmission especially when they are implemented by one or a hybrid of optical multiplexing techniques [3]. Among the techniques is (WDM) [4] which may be supported by DP multiplexing and space-division multiplexing (SDM) [5]. In the WDM system, different data streams are sent simultaneously on the same fiber after modulating each stream with different wavelength optical carriers, one stream for each carrier. Therefore, WDM is sometimes called optical frequency-division multiplexing. The WDM technology enables increasing level (see the complexity) of electronic-to-optical conversion (EOC) and optical-to-electronic conversion (OEC) [6]. Thus, WDM would lead to a data rate that is far higher than what can be handled by optoelectronic senders and receivers.

In conventional WDM systems, a bank of lasers is used at the transmitter side to provide the unmodulated optical carriers for the channels. The frequency of these lasers should be controlled to a high degree of accuracy to yield specific channel frequency spacing [7,8]. This frequency control reduces the stability and robustness and increases the cost of the system. In addition, a similar bank of lasers should be used at the receiver side when coherent detection is used to recover the data. To overcome this limitation, researchers have proposed to use an OFCG to replace the bank of lasers in WDM systems [9,10]. The OFCG is excited by a single continuous-wave (CW) laser and produces equally spaced optical lines that can be used as optical carriers for the WDM channels. Both direct detection [11] and coherent detection [12] optical frequency comb (OFC)-based WDM systems have been reported in the work. The results show that these systems are more robust, and less costly compared with conventional counterparts even when the WDM scheme is supported with SDM [13]. Further, one (or more) of the transmitter comb lines may be used as a pilot and sent without modulation over the fiber link to synchronize the receiver local OFCG [9].

Generally, an optical communication channel carrying a comb-based WDM system is called a superchannel since its operation depends on a single laser at the transmitter side. Recently, Mazur et al. [12] demonstrated 12 Tbps throughputs after 80 km transmission over a standard single-mode fiber (SSMF). Both DP 64-quadrature amplitude modulation (QAM) and 52-line superchannel from a single C-band 22 GHz line spacing soliton microcomb wave were used in their experiments. Further, Kong et al [13] demonstrated the transmission of 909.5 Tbps over 7.9 km 37-core fiber using 99-line WDM per fiber core and 64-QAM modulation format. They used a 50 GHz line spacing comb based on highly nonlinear fibers (HNLFs) which generate 99 lines across the C band.

The capacity of the superchannel depends on OFCG parameters, namely the number of optical lines N_{ch} and line frequency spacing Δf , modulation order M of the used M -QAM format, and the symbol rate R_s . The parameter R_s is measured by the unit of symbol per second (Sps) which is also called baud (Bd). Further R_s should be chosen less than Δf to prevent spectral overlapping between

successive modulated optical lines. The total transmission data by a single-polarization superchannel is equal to $N_{ch} \times R_s \times \text{Log}2M$. Note that both N_{ch} and R_s increase linearly the system capacity. This linear dependence does not apply to the modulation order M . Using 128-QAM to replace 64-QAM as a modulation format will enhance the capacity by $(\text{Log}2 128) / (\text{Log}2 64) = 7/6 = 1.17$. Therefore, to enhance the capacity of the superchannel, the comb should be designed to offer a large number of optical lines N_{ch} with large line spacing Δf . In general, most of the OFCGs reported in the research were either designed using HNLFs or optoelectronic modulators (EOMs) [14]. The fiber-based comb is relatively bulky but it's able to generate a large number of lines and a wide spectrum. In contrast, the EOM-based combs are characterized by their smaller size and higher robustness but it offers a lower number of lines. Further, the EOM-based comb can be integrated yielding (i.e., implemented in integrated optic or integrated electrooptic environment) chip comb [15]. These features make the EOM-based comb is more attractive for use in implementing WDM transmission compared with a fiber-based comb. The challenge facing research is to design a broadband EOM-based comb that offers a large $N_{ch}-\Delta f$ product. This issue is addressed in this work where an EOM-based comb configuration is proposed to yield 39 lines with 1 dB flattens and 150 GHz frequency spacing. The proposed comb will be used to design UWB WDM systems.

II. CONCEPTS OF USING OFCG IN COMMUNICATION SYSTEMS

An OFC can be defined as a series of equally spaced discrete optical spectral lines. Many parameters could be used to characterize the output of the OFCG such as the number of lines, line frequency spacing, occupied bandwidth, spectral flatness, frequency and amplitude stability, and phase noise [1]. Ideal OFCGs produce equal-power lines; but due to the bandwidth limitation of the used components, the power of the lines decreases as one moves far from the centreline. The OFCG can be treated as a multiwavelength optical source driven by a single CW laser. In other words, the OFCG behaves as a single-to-multiwavelength converter. The serial spectral lines that appeared at the comb output can be separated using an optical demultiplexer as shown in Figure 1. Thus, cascading the OFCG with optical demultiplexer generates a bank of optical lines which are equivalent to a bank of lasers. This makes the OFCG-demultiplexer configuration an efficient and compact optical WDM source compared with the conventional laser bank.

In a comb-based WDM system, each of the demultiplexed comb lines can be treated as an optical carrier to be modulated by the data of one of the WDM channels [2,3]. Generally, QAM is used where the data is embedded on both amplitude and phase of optical line waveform [3]. To illustrate that, consider the electric field of the i_{th} line $e_i(t) = E_i(t)\cos(\omega_i t + \theta_i t)$. Here $\omega_i = 2\pi f_i$ is the radian frequency of the i_{th} line. Further, $E_i(t)$ and $\theta_i(t)$ are the amplitude and phase which are modulated by the data. The field $e_i(t)$ can be expressed as $e_i(t) = I(t)\cos\omega_i t + Q(t)\sin\omega_i t$ where $I(t) = E(i)\cos\theta_i$ is called the in-phase component (I) and $Q(t) = E(i)\sin\theta_i$ which is called the quadrature (Q) component. Note that the QAM format can be considered as two amplitude modulation formats, one is the $\cos\omega_i t$ and the other on the quadrature carrier $\sin\omega_i t$. Therefore, the QAM signal is generated (detected) using IQ modulator (demodulator) in the channel transmitter (receiver).

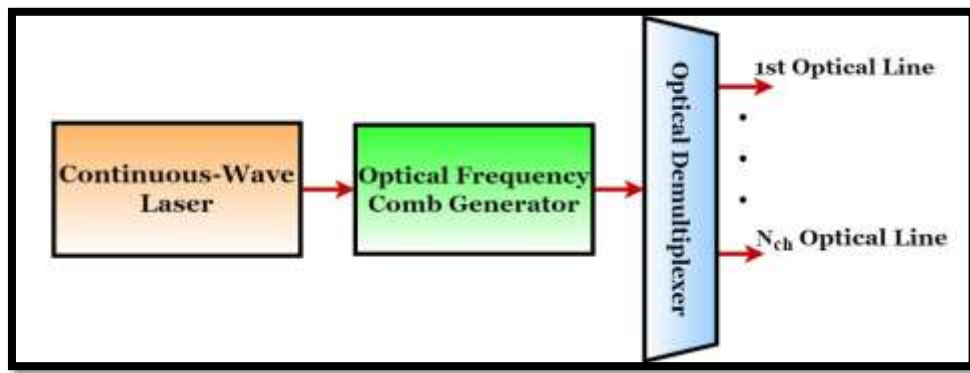


Fig1: Comb-based WDM optical source.

III. RELATED WORK

A- Related Work to Comb-based WDM Transmission

In 2016, Fülöp et al. [16] established that microresonator OFCGs meet the requirements for usage as WDM light sources in transmission networks longer than 100 km. The encoded data using DP-quadrature phase shift keying (QPSK) at 12.5 Gbaud on seven neighboring channels and successfully transmitted it over a recirculating fiber loop of more than 6000 km. This is the first demonstration of a Complementary Metal Oxide Semiconductors (CMOS)-compatible multiwavelength light source with long-haul coherent communications performance.

In 2017, Lie et al. [17] experimentally proposed and evaluated a recirculating frequency shifting (RFS) optical comb

optimization approach for terabit flexible optical networks. By dropping the erbium-doped-fiber amplifier (EDFA) gain in the shifting loop and installing an in-loop noise suppression filter, they achieve a higher OSNR with good stability (no system outage). They demonstrated that this source can handle DP Nyquist-16QAM transmission at 20x200 Gbps.

In 2018, Mazur et al. [10] demonstrated transmission of a comb-based 10 Tbps 50×20 Gbaud DP 64-QAM superchannel over 80 km SSMF using frequency comb regeneration at the receiver side to reduce carrier offsets and allow for self-homodyne detection. The regeneration was enabled by transmitting two optical pilot tones which were filtered and recovered in the receiver using optical injection locking and an electrical phase-locked loop.

In 2019, Marin-Palomo et al. [18] conducted WDM transmission using a chip-scale comb based on a quantum-dash (QD) mode-locked laser diode (MLLD). 75 km of SSMF, a DP 16-QAM WDM transmission on 38 channels was demonstrated with an aggregate net data rate of 10.68 Tbps.

In 2019, Mazur [7] Three 50×24 Gbaud DP 256-QAM superchannels were transmitted over the entire C band, with an overall SE of 12 b/s/Hz. A single shared optical pilot tone and a low-overhead pilot-based digital signal processing (DSP) are used in each comb-based superchannel.

In 2020, Corcoranu et al. [19] developed a microcomb based on soliton crystals to accomplish ultra-high data transmission over 75 km of SSMF. They demonstrated a line rate of 44.2 Tbps with a SE of 10.4 b/s/Hz in the telecommunications C band at 1550 nm.

In 2021, Mazur et al. [12] used a single 22 GHz line spacing soliton microcomb to create a 52-line superchannel. The findings of the experiment reveal that after 80 km of transmission, 12 Tbps throughput with > 10 bits/s/Hz SE efficiency was achievable, and after 2100 km, 8 Tbps throughput (SE > 6 bits/s/Hz) was also possible to achieve.

In 2021, Prayoonpong et al. [20] They discovered that noise-corrupted comb lines can reduce the OSNR required for the comb by 9 dB when used as optical carriers at the transmitter side, and by 12 dB when used as a local oscillator at the receiver side, these results were obtained after a test on a 19.45-GHz-spaced comb generating 71 lines, using 18 Gbaud, 64-QAM subchannels at a SE of 10.6 b/s/Hz.

B- Related Work to Integrated and EOM-based Combs

In 2018, Lin et al. [21] demonstrated flexible frequency comb generation using silicon photonic dual-drive MZMs manufactured on CMOS technology. After one level of optical amplification, the on-chip comb contains five lines spaced at 20 GHz with a high tone-to-noise ratio of roughly 40 dB. With 16-GBd 32-QAM on five WDM channels, the back-to-back transmission achieved bit error rates (BERs) considerably below 2×10^{-2} , the threshold for 20% overhead FEC. Also tested was a seamless 800-Gbps superchannel using 5×20 GBd 16-QAM with BER below the 7% overhead FEC threshold of 3.8×10^{-3} was tested.

In 2019, Wang et al. [22] implemented flexible on-chip OFCG in silicon photonics, using two cascaded EO-MZMs exhibited. It was possible to create a quasi-rectangular OFC with 9 lines and a comb spacing of up to 10 GHz with an amplitude variation (comb flatness) within 6.5 dB. Sinc-shaped Nyquist pulses with a full-width at half maximal duration as short as 11.4 ps have a satisfactory fit with the associated time-domain waveforms.

In 2020 Anashkina and Andrianoy [23] demonstrated OFCG in a silica microsphere with a zero-dispersion wavelength near 1550 nm the comb was pumped by a CW laser and it's broadly tunable in C band was investigated experimentally and theoretically.

In 2020, Buscaino et al. [24] investigated a canonical ring-based resonator-enhanced electro-optic (RE-EO) comb. They analyzed the effect of input optical phase noise and modulation phase noise affecting the comb that resulted. In the presence of dispersive waveguides, numerical models were also constructed to estimate the output spectrum. A dual-ring RE-EO comb was analyzed using these realistic models, and the results revealed that utilizing a small coupling ring can enhance conversion efficiency to 32%, compared to 1.3 % for a single-ring RE-EO comb generator.

In 2020, Ullah [25] presented a new technology based on serial cascading of a phase modulator and a dual-driven Lithium-Niobate MZM (DD-LiNbO₃-MZM) for the creation of UWB and flattened OFC. By carefully regulating the RF switching voltage of the DD-LiNbO₃-MZM and the signal frequency of the sinusoidal wave (RF) source, over 60 carriers were generated. To generate the greatest number of carriers, the frequency spacing was fixed at 20 GHz.

In 2021, Francis et al. [26] presented all-optical modulation of nanophotonic structures as a method for producing OFC. To describe cascaded all-optical photonic crystal intensity and phase modulators, a theoretical model based on temporal coupled mode theory was created. A separate carrier light is modulated using a modulation light with a sinusoidal waveform to generate an OFC. A flat OFC that spans 600 GHz was achieved by manipulating modulation power and device dimensions.

In 2021, Daniel et al. [27] investigated two distinct on-chip OFC architectures based on silicon EOMs. The goal was to create a flat tunable comb that could be used for optical integration on a silicon photonics platform. Within a 2 dB flatness, a total of nine lines were achieved, with line spacing ranging from 0.1 to 7 GHz.

It is clear from both parts of the related works that the EOM-based comb still attracts increasing interest due to its small size which makes it suitable for the integrated optic platform. However, more research is needed to design such comb type to offer a simultaneously high number of lines and large line spacing to support wideband high-capacity WDM systems. This issue will be addressed in this work.

IV. DESIGN AND PERFORMANCE INVESTIGATION OF UWB OFCG FOR WDM APPLICATIONS

In this section, a new compact, UWB EOM-based OFCG is proposed to replace a laser bank in WDM communication systems. The configuration uses two parallel MZMs in cascade with an EAM and can produce 39 lines within a 1dB-flattened spectrum. A single-RF source is used to control comb line spacing Δf without affecting the number of lines. Mathematical modeling is presented to describe the working principles of the proposed comb. Further, the spectral characteristics of the comb are simulated for different values of Δf (25, 50, 100..., and 150 GHz) using Optisystem software ver.15. Finally, the proposed comb is used as a basic unit to design 0.5 dB-flatness 72-line comb to support extended C-band WDM system.

Design of UWB OFCG

A- Design Requirements and Proposed Comb Configurations: Certain requirements are needed to be satisfied in designing UWB comb for advanced WDM communication systems. Among these requirements are

- (i) The comb should have high robustness, a small size, and low-energy consumption. Therefore, the proposed design in this work is based on EOMs and can be used to produce an in-chip comb.
- (ii) The comb lines should have the same state of polarization (SOP) and frequency spacing Δf which is useful for the DP-WDM system. In the proposed design, the center frequency of the comb spectrum and SOP of its lines are controlled by the CW laser center frequency and SOP of the seed WDM, respectively.
- (iii) The line frequency spacing can be tuned by a minimum number of devices. In this work, a single RF oscillator is used for tuning Δf up to 200GHz.
- (iv) The configuration should be simple, flexible, and adaptive. The proposed design enables the operation in C, L, and C+L bands.
- (v) The comb should produce many flattened optical lines.

According to these requirements, the configuration of the proposed UWB comb is constructed according to the schematic shown in Figure 2. The configuration consists mainly of two parallel MZM modulators whose combined outputs are injected into an EAM. The configuration is driven by two sinusoidal signals, namely an optical signal coming from the CW laser and RF signal from the RF oscillator. The configuration uses a single RF source for tuning Δf . Further, the EAM is inserted at the last stage of the design since this modulator type is characterized by an UWB bandwidth and therefore, can cooperate efficiently with the input of the combined-MZMs output signal. The proposed configuration is initially simulated many times using Optisystem software ver.15 to deduce the values of the proper parameters and operating conditions of the used EOMs that yield as many flattened lines as possible. The initial tests end with the following findings

- (i) Both MZMs operate in a single-drive (SD) push-pull (PP) mode.
- (ii) The RF signal is applied to MZM1 and EAM only. Therefore, MZM2 is subject only to a bias voltage and not driven by the RF signal.
- (iii) Both bias voltage and the amplitude of the RF signal applied to MZM1 are set $V_{\pi}/2$. The bias voltage for MZM2 is set to V_{π} .
- (iv) The EAM operates with a modulation index of 0.5.

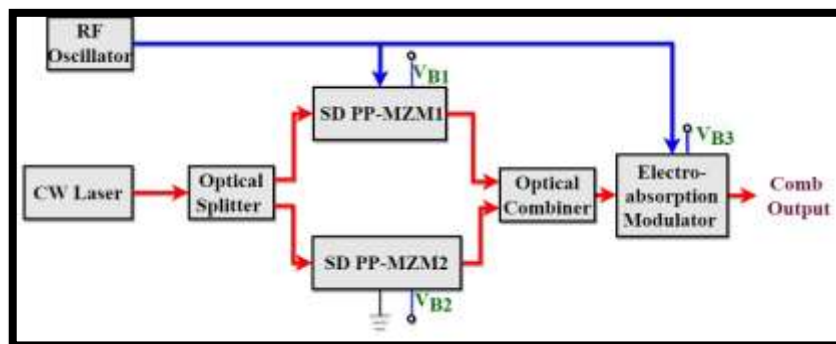


Fig 2: Generalised block diagram of the proposed UWB comb.
SD PP-MZM: Single Drive push-pull Mach-Zehnder Modulator.

b- Mathematical Framework: This subsection presents a mathematical model to describe the comb output spectrum and address the key role played by each modulator. The analysis is introduced under the following assumptions

- (i) Both MZMs have identical structures and internal-device parameters including the switching voltage V_{π}
- (ii) Both MZMs operate in SD PP mode.
- (iii) The power splitting ratio of the beam splitter = 0.5 (i.e., 3dB-splitter).
- (iv) All the used photonic devices are lossless.

Note that the developed model can be extended easily for cases where one or more of these assumptions are not valid.

The SD PP-MZM is characterized by $\Phi_{av} = 0$ and therefore, the relation between input field $e_{in}(t)$ and output field $e_{out}(t)$ can be deduced from eqn. $E_{out} = E_{in} (\cos\Phi_{av} + j\sin\Phi_{av}) \cos(\Delta\Phi/2)$ as

$$e_{out}(t) = e_{in}(t) \cos\theta \quad (1)$$

where $\theta = \Delta\Phi/2$. Let the total voltage $v(t)$ applied to the MZM consist of a DC component V_B and an RF signal $v_{RF}(t) = V_{RF} \sin\omega_{RF}t$. Then the introduced phase modulation θ is given by

$$\theta = \frac{\pi V(t)}{V_\pi} = K(1+m \cos\omega_{RF}t) \quad (2)$$

where $K = \pi V_B/V_{RF}$ and m is the modulation index $m = V_{RF}/V_B$.

Using eqn. 2 into eqn. 1 yields

$$e_{out}(t) = e_{in}(t) \cos(K + mK \cos\omega_{RF}t) \\ = e_{in}(t) (\cos K \cdot \cos(mK \cos\omega_{RF}t) - \sin K \cdot \sin(mK \cos\omega_{RF}t)) \quad (3)$$

Using the following two Bessel's identities [28]

$$\cos(z \cos\theta) = J_0(z) + z \sum_{n=1}^{\infty} (-1)^n j_{2n}(z) \cos(2n\theta) \\ \sin(z \cos\theta) = -z \sum_{n=1}^{\infty} (-1)^n j_{2n-1}(z) \cos[(2n-1)\theta]$$

where J_n is the n th Bessel function of the first kind) into eqn. 3 yields

$$e_{out}(t) = s_m(t) e_{in}(t) \quad (4a)$$

$$e_{out}(t) = e_{in}(t) [A_0 + \sum_{n=1}^{\infty} A_n \cos(2n\omega_{RF}t) + B_n \cos[(2n-1)\omega_{RF}t]] \quad (4b)$$

where

$$A_0 = J_0(mK) \cos K \quad (5a)$$

$$A_n = 2(-1)^n J_{2n}(mK) \cos K \quad (5b)$$

$$B_n = -2 J_{2n-1}(mK) \sin K \quad (5c)$$

Investigating eqn. 4 reveals the following facts

- (i) The terms containing the Bessel functions $s_m(t)$ can be considered as a modulating signal used to modulate the amplitude of the amplitude signal $e_{in}(t) = E_{in} \cos(\omega_0 t)$. Here ω_0 presents the optical frequency of the CW laser.
- (ii) The modulating signal contains a DC component of A_0 value, even harmonics of frequency $2n\omega_{RF}t$ and amplitude A_n , and odd harmonics of frequency $(2n-1)\omega_{RF}$ and amplitude B_n .
- (iii) Modulating the optical field by any discrete components of the modulating signal produces upper- and -lower sidebands around ω_0 . Thus the comb spectrum is discrete and contains the frequencies

$$\omega_0, \omega_0 \pm \omega_{RF}, \omega_0 \pm 2\omega_{RF} \dots$$

with amplitudes $A_0, B_1/2, A_1/2 \dots$ respectively.

$$\text{One can use eqn. } \frac{I_{out}}{I_{in}} = \frac{|E_{out}|^2}{|E_{in}|^2} = (\cos^2\Phi_{av} + \sin^2\Phi_{av}) \cos^2(\Delta\Phi/2)$$

$= \cos^2(\Delta\Phi/2)$ to find the field $e_c(t)$ at the output of the combiner. The field $e_c(t)$ is equal to $(1/\sqrt{2})$ x sum of the two MZMs output fields. Let the parameters of MZM1 and MZM2 be distinguished in the following analysis by using the subscripts $i = 1$ and 2 , respectively. Let the input field of the comb is given by $e_{in}(t) = E \cos\omega_0 t$, and the applied total voltage is given by

$$v_i(t) = V_{Bi} (1+m \cos\omega_{RF}t) \quad i = 1,2 \quad (6)$$

where $m_i = V_{RFi}/V_{Bi}$. The combined optical signal field can be expressed as

$$e_c(t) = 0.5 [\sum_{i=1}^2 s_{mi}(t)] e_{in}(t) \quad (7)$$

The coefficient 0.5 comes from the assumption of using 3dB-splitter which divides equally the input field to the two output ports with $e_{in}(t)/\sqrt{2}$ field going to each output port. The two modulating signals $s_{m1}(t)$ and $s_{m2}(t)$ correspond to MZM1 and MZM2 respectively, and they are calculated by using eqn. 4b.

Note that the two MZMs have the same discrete frequencies at their output spectra and therefore, one can use their parameters $K = V_{Bi}/V_\pi$ and $m = V_{RF}/V_B$ to control the flattens of the combined spectrum. According to eqn. 7 the combined field $e_c(t)$ indicates that the comb input field $e_i(t)$ is amplitude modulated by a combined modulating signal $s_{mc}(t) = s_{m1}(t) + s_{m2}(t)$.

$$e_c(t) = 0.5 s_{mc}(t) e_{in}(t) \quad (8a)$$

$$s_{mc}(t) = a_0 + \sum_{n=1}^{\infty} a_n \cos(2\pi\omega_{RF}t) + b_n \cos[2\pi(2m-1)\omega_{RF}t] \quad (8b)$$

where $a_0 = A_{01} + A_{02}$, $a_n = A_{n1} + A_{n2}$, and $b_n = B_{n1} + B_{n2}$.

The optical electric field $e_c(t)$ will pass through the EAM to obtain a wide-bandwidth comb out spectrum. Generally, the EAM modulator produces the output field proportional to the square root of the applied electrical signal. Since the square root of the operation is a nonlinear one, a wide spectrum is expected at EAM output due to generation of many sidebands related to the

applied electrical signal and its harmonics. In this work, the relation between input and output fields of the EAM is taken from Ref. [29] and adopted here according to the used symbols. The EAM is assumed driven by the signal $v_s(t)$

$$\begin{aligned}
 V_s(t) &= V_{B3} + V_{RF3} \cos(\omega_{RF}t) \\
 &= V_{B3}[1 + m_3 \cos(\omega_{RF}t)]
 \end{aligned}
 \tag{9}$$

where $m_3 = V_{RF3}/V_{B3}$.

The output field of the EAM (i.e., the comb) is given by

$$e_{out}(t) = t_{EAM} e_c(t) (\sqrt{x(t)} e^{j0.5\alpha \ln(x(t))}) e_c(t)
 \tag{10a}$$

where t_{EAM} is the field transmission coefficient of the modulator, α is the chirp factor of the modulator, and

$$x(t) = (1 - m) + m \cos(\omega_{RF}t)
 \tag{10b}$$

Here $m = (1 - m_3)/(1 + m_3)$ is the effective modulation index of the EAM.

Combining eqns. 7 and 10a yields the relation between the input and output field of the comb

$$e_{out}(t) = [\sum_{i=1}^2 s_{mi}(t)] t_{EAM} \cdot e_{in}(t)
 \tag{11}$$

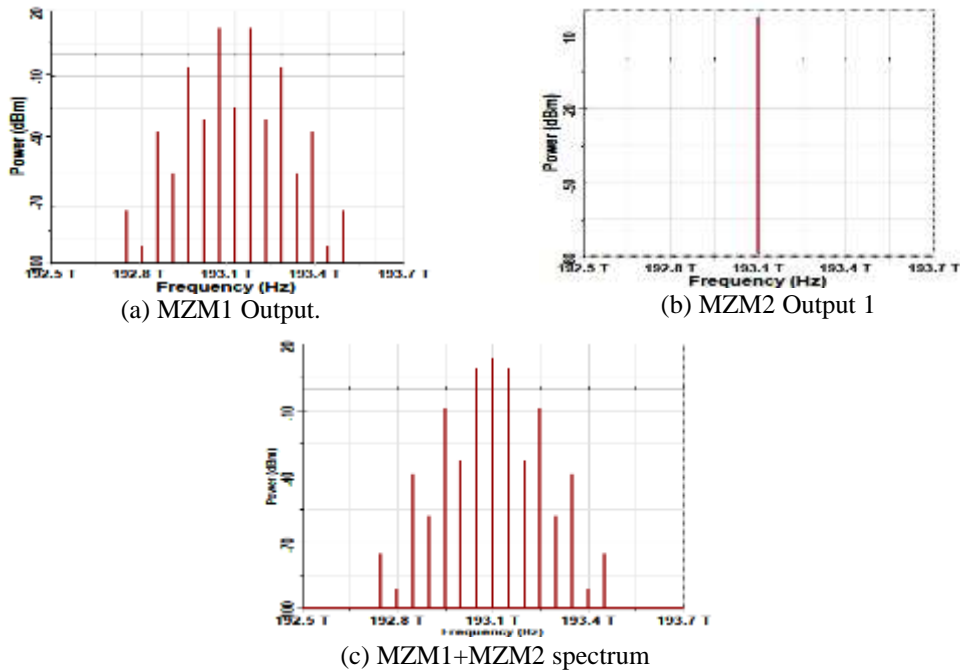
Simulation Results Characterizing the Proposed Comb Spectrum

The proposed OFCG is implemented in Optisystem software ver.15 environment to simulate its spectrum characteristics. The parameters of the electric driven signals (DC + RF amplitude) for the three modulators are selected, after trial and error, to achieve a flattened spectrum with a maximum number of comb lines with 3dB flatness. The final design ends with the following parameters

- (i) MZM1 is driven by a bias $V_{B1} = V_{\pi}/2$ and RF signal having a modulation index $m_1 = 1$.
- (ii) MZM2 is driven only by a DC voltage $V_{B2} = V_{\pi}$. The output field and input field of this modulator are related $e_{out}(t) = e_{in}(t) \cdot \cos(\pi V_B/V_{\pi})$ which leads to $e_{out}(t) = -e_{in}(t)$ when $V_B = V_{\pi}$.
- (iii) The parameters of EAM are effective modulation index $m = 0.5$ and chirp factor $\alpha = 125$.

The simulation results are presented for the ideal case of lossless EOMs and when the OFCG is driven by a 20 dB CW laser operating at 193.1 THz frequency (i.e., $\lambda = 1154$ nm). The effect of EOMs losses and CW laser power of comb spectrum will be discussed later.

Figure 3 illustrates the signal spectrum at different points of the Comb configuration when $f_{RF} = 50$ GHz. Parts a-d of this figure show the spectrum at the MZM1 output, MZM2 output, combiner output, and comb output. Part e of this Figure shows the 3dB-flatness spectrum of the comb output. Note that although MZM2 produces a single-line spectrum it's useful to support the power of the same frequency components generated by MZM1. Figure 3 e indicates that the comb generates 39 lines within 1dB flatness.



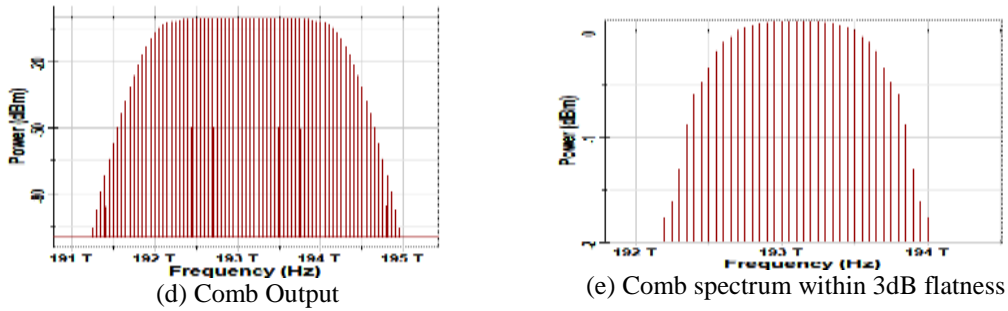


Fig 3: Signal spectrum at different points of the comb configuration when $f_{RF} = 50\text{GHz}$.

Note further that all the comb lines are equally spaced with $f_{RF} = 50\text{GHz}$ frequency separation. Table I lists the frequencies and power of comb lines when the device operates with 193.1 THz laser of 20 dBm power and 50 GHz RF signal. Note that the comb output spectrum is symmetric about a central line corresponding to $f = 193.1\text{ THz}$ which is the same frequency of the CW laser. This comb line is labeled here by the number 0 while, positive and negative integers are used for other comb lines when their frequencies are above or below 193.1 THz, respectively. From Table I one can deduce the number of comb lines for a given flatness and the results are depicted in Figure 3. The OFCG has 25 and 31 lines within 0.5 and 1dB flatness, respectively.

The comb spectrum is also simulated for different values of RF frequency and the results are displayed in Figs 4 a-g for $f_{RF} = 25, 50, \dots, 150\text{ GHz}$, respectively. Each Figure contains two spectrum pictures corresponding to the complete spectrum and 3dB-Flatness spectrum. Note that the RF frequency controls the line frequency spacing leading to $\Delta f = f_{RF}$. In contrast, the number of comb lines and their power is not affected by the RF frequency.

Further, to investigate the insertion losses IL of the comb and address the effect of laser power on the power level of the comb lines. The insertion loss is computed from

$$IL = \frac{P_{in}}{P_{out}} = \frac{P_i}{\sum_n P_n} \quad (12a)$$

$$IL_{dB} = 10 \log(IL) \quad (12b)$$

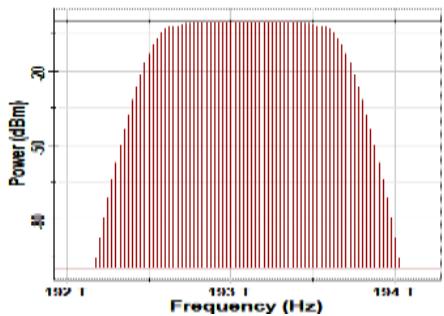
where P_{in} and P_{out} are the input and output power of the comb, respectively, and P_{in} denotes the power of the n_{th} comb line. The summation in eqn. 12a is carried out over all the comb output lines. From Table I, $P_{out} \approx 43.35\text{ mW}$ when $P_{in} = 100\text{ mW}$ (20 dBm). This leads to $IL = 100/43.35 = 2.3$ and therefore, $IL_{dB} = 3.6\text{ dB}$. Note that the power of the comb lines located within 3dB flatness shares about 0.75 of the total output comb power.

Since nonlinear optics associated with the comb elements is assumed negligible, one expects that the power of each comb line scales linearly with the laser power. This is evident from the results reported in Figs. 5 and 6. In Fig.5, the comb spectrum is plotted when the laser power is reduced from 20 dBm to 17 dBm (50mW) while f_{RF} is kept fixed at 50 GHz. Comparing the spectra of Figs 3 and 5 reveals that the power of each comb line reduces to half as the laser power changes from 100 mW to 50 mW. Note that the normalized comb spectrum, which reflects P_n/P_{out} , does not affect by the laser power. The dependence of central line power P_o on laser power P_{laser} is illustrated in Figure 6. The linear relation between P_o and P_{laser} is clear in this Figure.

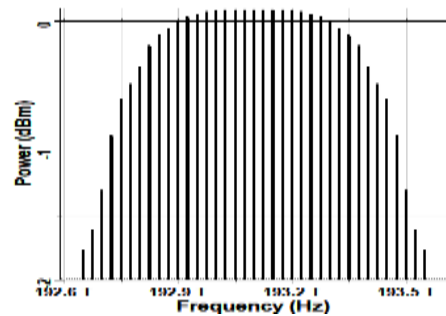
Table I Frequencies and powers of the optical comb lines generated by the proposed comb when it is designed with 20dBm-193.1 THz laser and laser and $\Delta f = 50\text{ GHz}$.

Line Number	Frequency (THz)	Power (dBm)	Line Number	Frequency(THz)	Power (dBm)
-37	191.25	-95.68	1	193.15	0.09
-36	191.3	-87.45	2	193.2	0.09
-35	191.35	-79.46	3	193.25	0.09
-34	191.4	-71.74	4	193.3	0.08
-33	191.45	-64.29	5	193.35	0.08
-32	191.5	-57.14	6	193.4	0.06
-31	191.55	-50.30	7	193.45	0.04
-30	191.6	-43.79	8	193.5	0.01
-29	191.65	-37.62	9	193.55	-0.05
-28	191.7	-31.84	10	193.6	-0.11
-27	191.75	-26.45	11	193.65	-0.18
-26	191.8	-21.50	12	193.7	-0.34
-25	191.85	-17.01	13	193.75	-0.48
-24	191.9	-13.02	14	193.8	-0.60
-23	191.95	-9.58	15	193.85	-0.88
-22	192	-6.73	16	193.9	-1.31

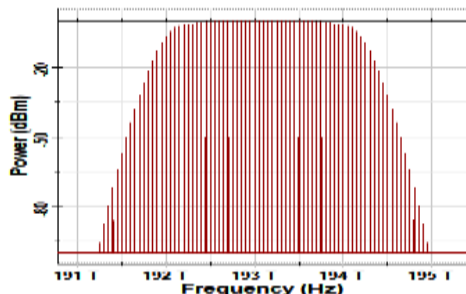
-21	192.05	-4.52	17	193.95	-1.61
-20	192.1	-2.99	18	194	-1.77
-19	192.15	-2.12	19	194.05	-2.12
-18	192.2	-1.77	20	194.1	-2.99
-17	192.25	-1.61	21	194.15	-4.52
-16	192.3	-1.31	22	194.2	-6.73
-15	192.35	-0.88	23	194.25	-9.58
-14	192.4	-0.60	24	194.3	-13.02
-13	192.45	-0.48	25	194.35	-17.01
-12	192.5	-0.34	26	194.4	-21.50
-11	192.55	-0.18	27	194.45	-26.45
-10	192.6	-0.11	28	194.5	-31.84
-9	192.65	-0.05	29	194.55	-37.62
-8	192.7	0.01	30	194.6	-43.79
-7	192.75	0.04	31	194.65	-50.30
-6	192.8	0.06	32	194.7	-57.14
-5	192.85	0.08	33	194.75	-64.29
-4	192.9	0.08	34	194.8	-71.74
-3	192.95	0.09	35	194.85	-79.46
-2	193	0.09	36	194.9	-87.45
-1	193.05	0.09	37	194.95	-95.68
0	193.1	0.09			



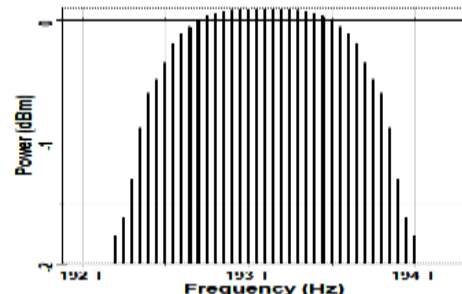
(a1) 25 GHz.



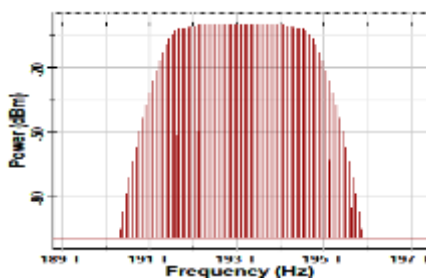
(a2) 25 GHz, 3dB.



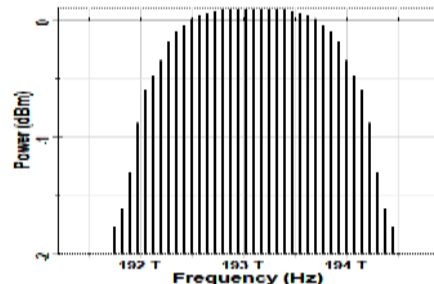
(b1) 50 GHz.



(b2) 50 GHz, 3db.

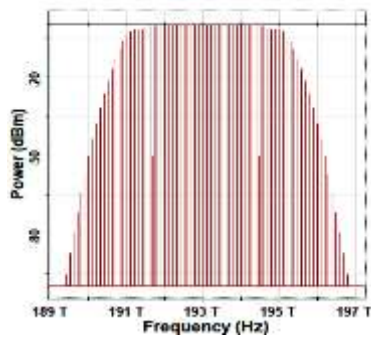


(c1)75GHz.

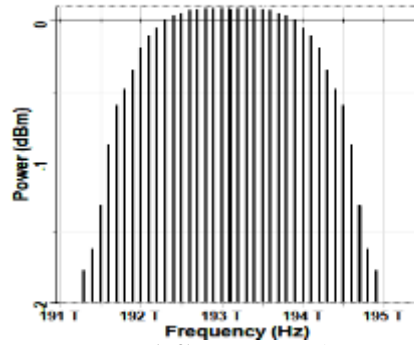


(c2)75GHz ,3dB.

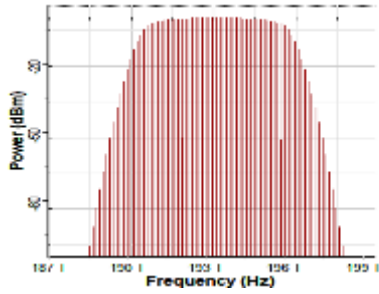
Fig 4: Comb spectrum for different values of RF frequency f_{RF} and assuming 20dB-193.1THz laser. Each part of the figure consists of two subparts which are distinguished by the subscript 1 and 2 to denote the complete and 3dB-flatness spectrum, respectively.



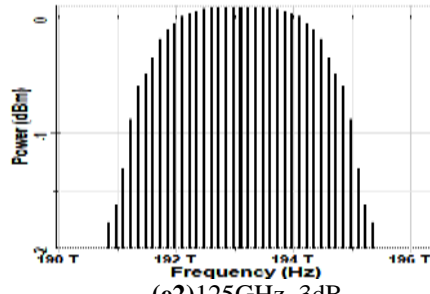
(d1) 100GHz.



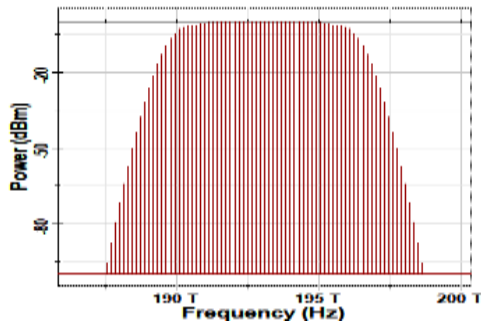
(d2) 100GHz ,3dB.



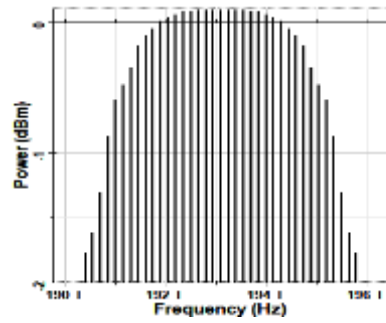
(e1) 125GHz.



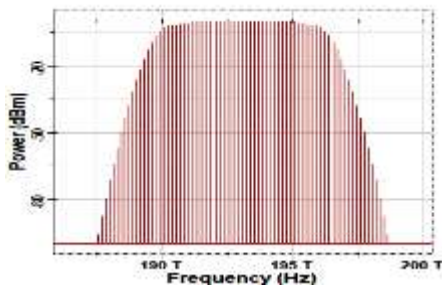
(e2) 125GHz ,3dB.



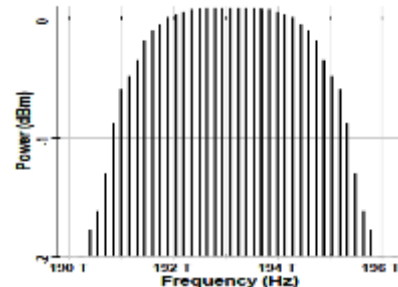
(f1) 150GHz.



(f2) 150GHz ,3dB.



(g1) 175GHz.



(g2) 175GHz ,3dB.

Fig 4: (Continued).

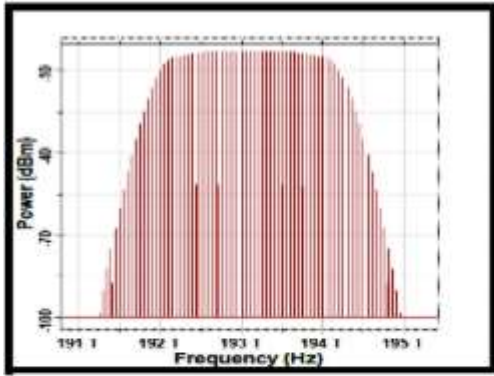


Fig 5: Comb spectrum when the laser power reduced to 17 dBm.

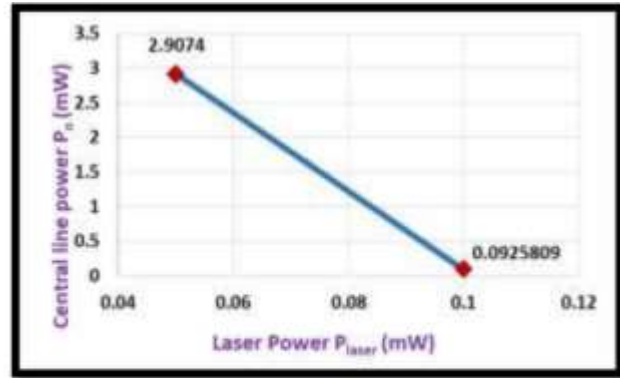


Fig 6: Dependence of central line power P_o on laser power P_{laser} for a comb designed with $\Delta f = 50\text{GHz}$.

Design of Broadband OFCGs Using the Proposed Comb as a Basic Unite

Broadband OFCGs are a key enabling technology for many applications including high-capacity dense wavelength-division multiplexing (DWDM) communication systems. In this section, the proposed comb will be used as a basic unit to develop two broadband OFCGs for DWDM systems one for C+L band and the other for the extended C band.

A- (C+L) Band Comb: The C band ranges from 1530nm to 1565nm and it is usually used in conventional WDM systems. To expand the capacity of terrestrial DWDM, an additional wavelength band immediately adjacent to the C band is used, namely the L band which ranges from 1565-1625 nm. This leads to C+L band transmission.

Figure 7 shows a schematic of C+L OFCG developed by exciting the proposed comb configuration by two CW lasers, i.e., C-band laser and L-band laser. The outputs of the two lasers are applied to an optical combiner and the resultant signal is launched to the comb unit. The optical comb procedures an output field $e_o = \frac{1}{\sqrt{2}} [e_{co}(t) + e_{Lo}(t)]$ where e_{co} and e_{Lo} is the output fields for C-band and L-band combs, respectively. Thus, from power point of view, $P_o = 0.5(P_{co} + P_{Lo})$. Thus are the power of each comb which is reduced by 3dB at the combiner output.

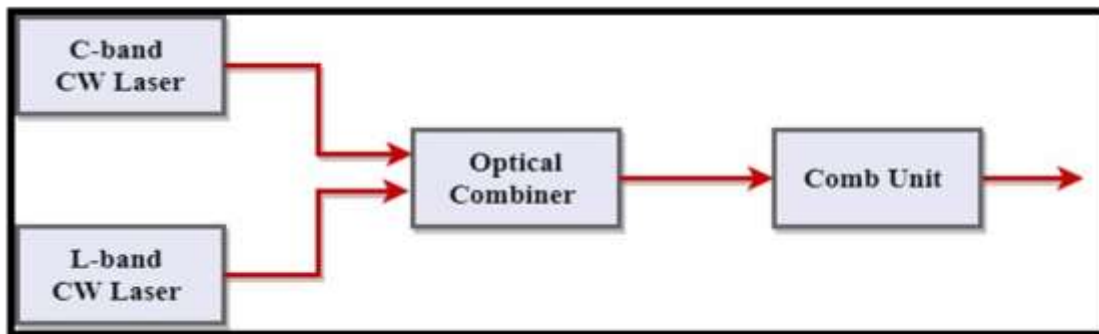


Fig 7: (C +L) band OFCG using the proposed comb unit.

The spectrum of the OFCG of Figure 7 is simulated for $\Delta f = 100\text{ GHz}$ using two 23 dB-power lasers, one operates at 188.4 THz (L band) and the other at 193.4 THz (C band). These two frequencies correspond to the middle channel in L and C bands, respectively, according to 50-channel, 100GHz. spacing IUT-T WDM grid. The corresponding wavelengths are approximately 1592.4 and 1551.2 nm, respectively. The simulation results are given in Figure 8 which shows the complete and 3dB-flatness spectrum of the comb output. Note that the 3dB-flatness spectrum reflects a two-band spectrum resulting from the addition of the two individual L and C bands spectra. Note further that both band's spectra appear uncorrelated having an identical number of lines and line power density. Further, the frequency separation between the two lasers is 5 THz which covers 50 lines with 100 GHz spacing. This frequency spectrum is more than 3.2 THz occupied by the 32 3 dB-flatness lines (16 lines above the 188.4 THz and 16 lines below the 193

THz). Thus the frequency separation between the edges of two 3dB-flatness spectra is $5 - 3.2 = 1.8$ THz which reduces the interaction between L and C band spectra.

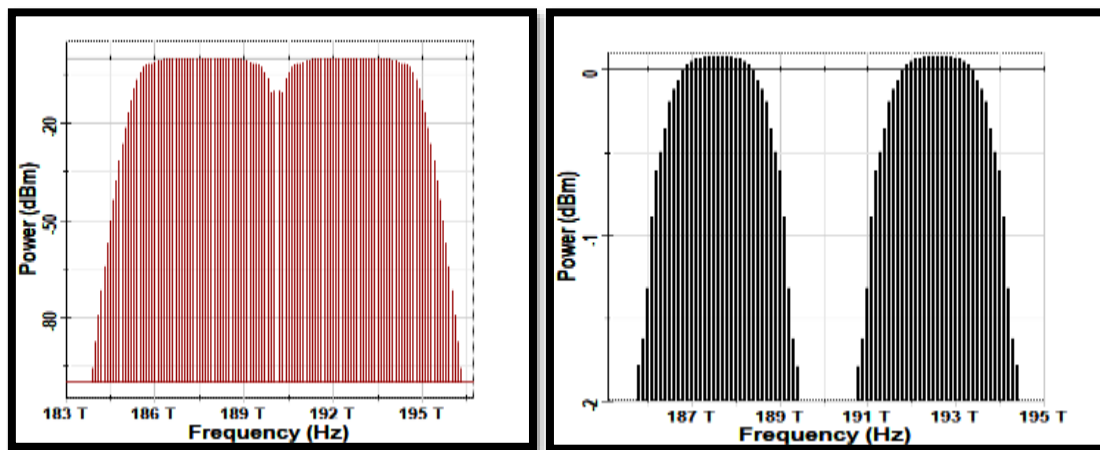


Fig 8: Complete and 3dB-flatness spectrum of the C+L comb output.

More investigation is carried out to address this point and the results indicate that reducing the lasers frequency separation to 4.7 THz increases the overlapping between L- and C- band spectra leading to undistinguishable 3dB-flattened spectra.

Design of 72-Line Comb for Extended C-band WDM System

The extended C-band WDM communication system uses the conventional C-band channels plus additional channels for the next neighbouring bands, L and S bands. The 72-channel extended C band uses $\Delta f = 100\text{GHz}$ and stars from 190.1 THz (Ch1) and ends with 197.2 THz (Ch72). This subsection aims to present a design and simulation results for a 72-line comb using the previously proposed OFCG as a basic unit and keeping the excitation from a single CW laser. The idea is to design a 24-line comb as a basic unit and use two of its extra lines to drive two 24-line combs of the same configuration. The extended C-band spectrum is divided into three 2.4 THz subbands, SB1-SB3. The three subbands cover the ranges 190.1-192.4 THz (Ch1-Ch24), 192.5-194.8 THz (Ch25-Ch48), and 194.9-197.2 THz (Ch49-Ch72). The central channels of these subbands are 191.3, 193.7, and 196.1 THz, respectively. Note that the basic comb unit produces 24 lines within 0.5 dB flatness (see Table I).

Figure 9 illustrates the configuration of the proposed 72-line comb which uses three 0.5dB-flatness 24-line combs. The first 24-line comb is driven by a 193.7 THz CW laser to produce the 24 lines of the middle subband, SB2. Each of the 191.3 THz and 196.1 THz comb lines is selected by an optical bandpass filter (OBPF) and then amplified by a 33dB-gain optical amplifier (OA) before using it to excite a 24-line comb corresponding to subbands SB1 and SB3, respectively. The 33 dB gain has been chosen to ensure that each of the three 24-line combs is driven by 20 dB optical signal. To reduce the effect of the amplified spontaneous emission noise introduced by the OA, an additional OBPA is inserted after the amplifier. The bandwidth of each of the four OBPFs used in the design is selected to be much less than 100 GHz since a single-frequency component is to be selected at its output.

It is worth mentioning here that the spectrum of each of the 24-line combs contains many lines including the required 24 lines. To reduce the overlapping between the three subband combs, the output of each of these is applied to a 1:24 optical demultiplexer to produce pure 24 lines. At this point, the design can be considered as a three-output port 72-line comb-demultiplexer and as shown in Figure 10 can be applied directly to the extended C-band WDM system. Each port offers 24 parallel optical carriers from the 72 extended C-band carriers. Further, the outputs of three demultiplexers may be applied to a 72:1 multiplexer to produce a 0.5 dB flatness 72-line comb.

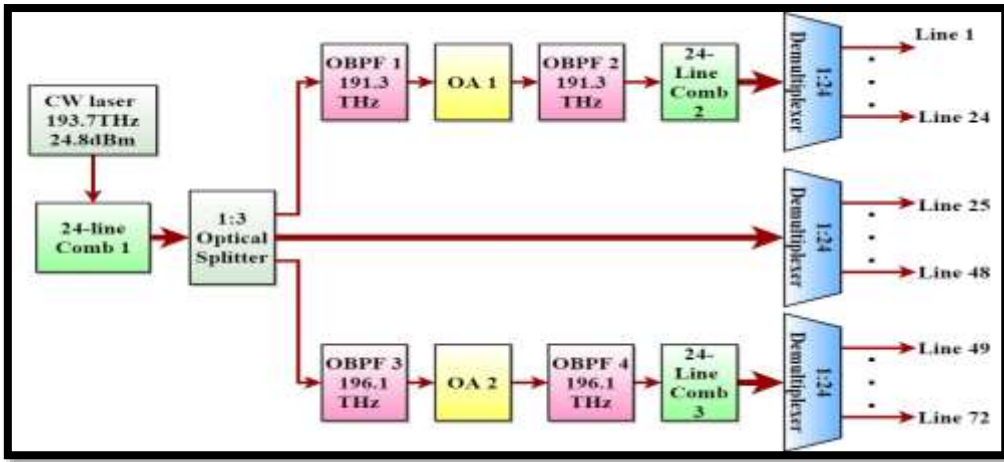


Fig 9: Configuration of the proposed 72-line comb for extended C-band WDM system operating with 100 GHz channel spacing.

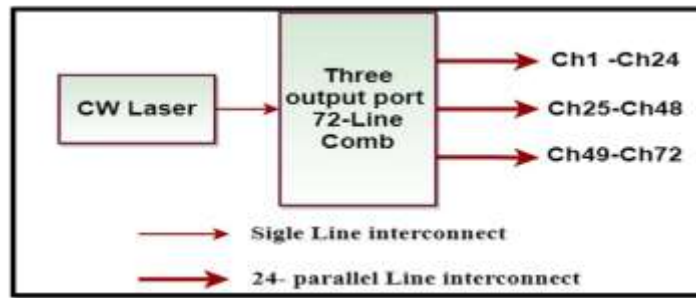
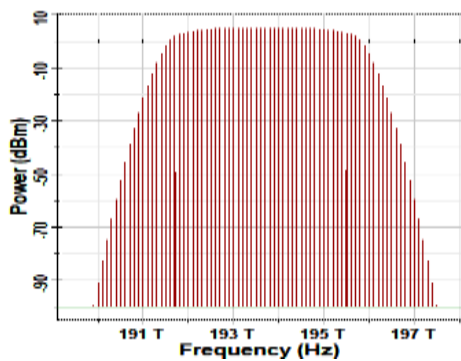


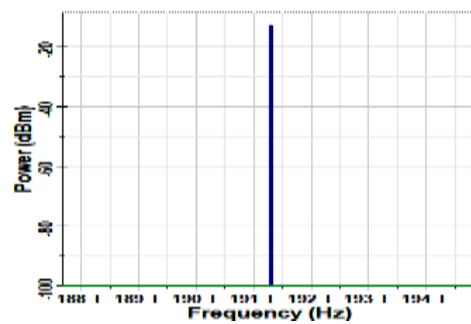
Fig 10: Three-output port 72-line comb-demultiplexer Configuration.

The spectral characteristics of the designed 72-line comb are simulated when it's driven by a 193.7 THz-CW laser of 24 dBm power and using 100 GHz RF frequency. The 1:3 optical splitter divides the output of the 24-line comb into three equal-power components with the central output port acting as a 24-line comb driven by 20 dBm laser. Further, the gain of each of the two amplifiers used in the upper and lower arms is set to 33 dB to make the corresponding 24-line combs (comb2 and comb3) appear as driven by a 20 dBm laser. The simulated results are displayed in Figure 11 which shows the signal spectrum at different points of the system. Parts a-e of this figure shows the spectrum at the outputs of the splitter central port, OBPF1, optical amplifier 1, comb2, and comb3, respectively. Note that the output of the two OAs contains the required optical frequency components embedded in amplified spontaneous emission noise. Further, the spectra of the output of comb2 and comb3 have identical power distribution and spectral shape as that of the central output port of the splitter. This is further illustrated in Figure 12 where the 3 dB-flatness spectrum is plotted for each of the three 24-line combs.

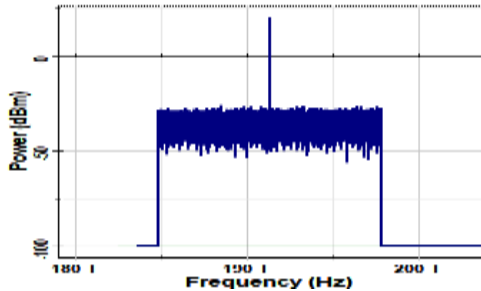


Spectrum of the central port of the beam splitter.

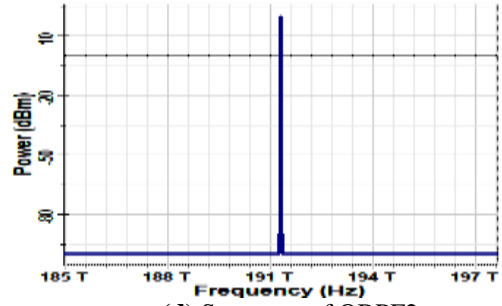
(a)



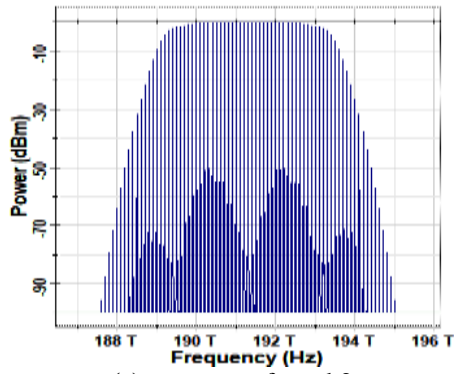
(b) Spectrum of OBPF1.



(c) Spectrum of OA1.

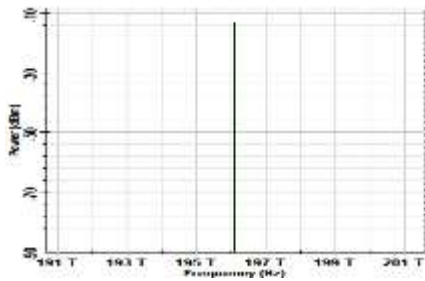


(d) Spectrum of OBPF2.

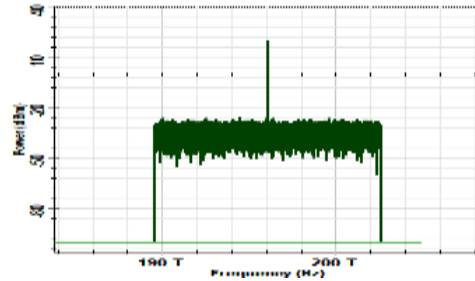


(e) spectrum of comb2.

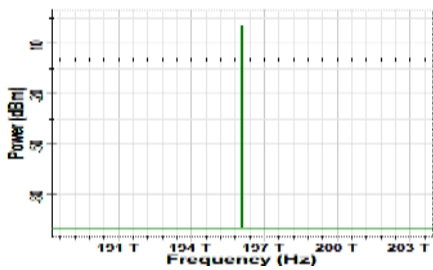
Fig 11: Signal spectrum at different points of the 72-line comb system.



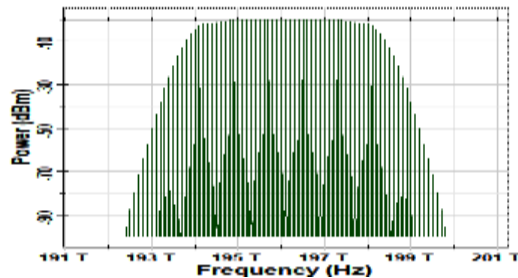
(f) Spectrum of OBPF3.



(g) Spectrum of OA2.



(h) Spectrum of OBPF2.



(i) spectrum of comb3.

Fig 11: (Continued).

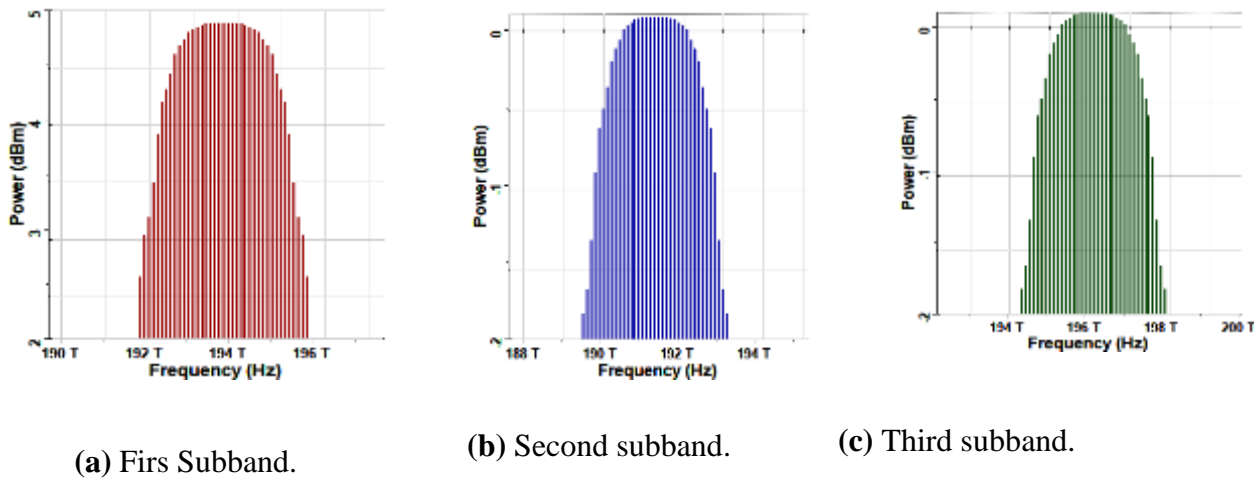


Fig 12: 3d dB-flatness spectrum of each of the three subbands generated by the designed 72-line comb.

V. TRANSMISSION PERFORMANCE OF WDM SYSTEMS INCORPORATING THE PROPOSED OFC CONFIGURATIONS

The designing of a coherent-detection WDM communication system requires the use of two identical laser banks, one for providing the channel optical carriers at the transmitter side and the other to act as optical local oscillator (LOs) at the receiver side. In this section, the OFC configurations proposed in the previous part are used to replace these two laser banks. The transmission performance of a WDM system designed with the proposed basic comb unit is investigated in the C band for different values of a number of channels N_{ch} (8, 16, and 32) and symbol rates R_s (40, 80, and 120 GSps) and assuming DP 16-QAM modulator format. Then, the performance of the WDM system incorporating the designed three-output port 72-line comb is evaluated for $R_s = 80$ GSps and DP 16-QAM format. The simulation is performed using Optisystem software ver.15.

Configuration and Design Concepts of the Investigated Comb-based WDM Transmission System

Figure 13 shows a simplified block diagram describing the coherent comb-based WDM system under investigation. At the transmitter side, the output of the comb is applied to $1:N_{ch}$ optical demultiplexer to select parallel N_{ch} lines to act as unmodulated optical carriers of the N_{ch} -channel WDM system. A bank of N_{ch} DP 16-QAM channel transmitter is used to embed N_{ch} data sequence on the selected N_{ch} comb lines (one data sequence per line). The modulated comb lines are applied to $N_{ch}:1$ optical multiplexer to generate the transmitter WDM signal. A booster optical amplifier (OA) is inserted at the output of the WDM transmitter to compensate its insertion loss and enhance the power of the optical signal launched to the fiber.

The transmission link consists of a number of spans N_{span} where each span has 80 km of standard single-mode fiber (SSMF) followed by an OA to compensate loss. In C band, the loss of the SSMF is almost 0.2 dB/km. The OA gain in decibel $G_{dB} = 0.2L_{span}$ where L_{span} is the length of the fiber span. Thus, a loss-compensated transmission link is assumed here. In contrast, these dispersion characteristics of the SSMF is wavelength dependent and hence DSP is used in each channel received to compensate this effect.

The received WDM signal is first applied to $1:N_{ch}$ optical demultiplexer to separate the individual channels which go through a bank of N_{ch} coherent DP 16-QAM channel receivers. The WDM receiver side also uses an OFCG identical to that used in the transmitter side to generate the N_{ch} local oscillator waveforms required for coherent optical detection. An OA may be inserted after the comb to enhance the power of the LO comb lines to achieve LO short-noise-limited detection process.

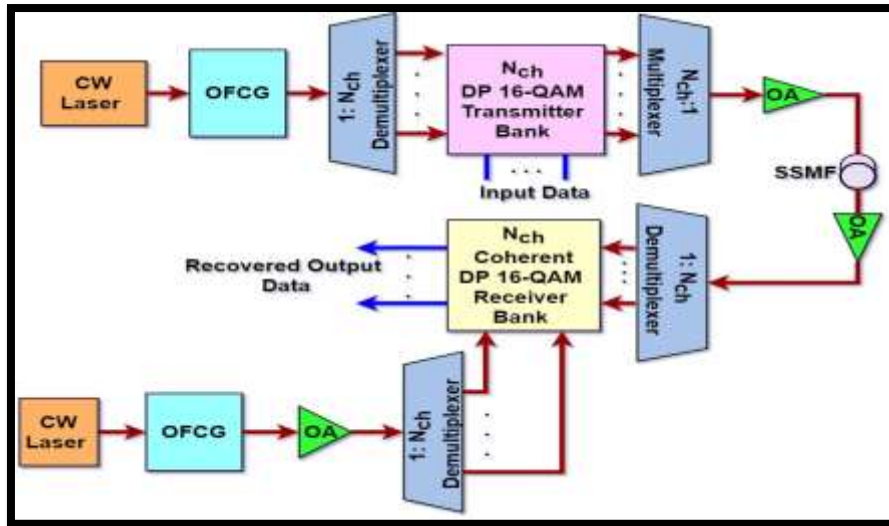


Fig 13: Simplified block diagram-describe of the investigated coherent comb-based WDM transmission system.

The following points should be kept in mind when designing the comb-based WDM under investigation

(i) The optical frequencies of the comb lines should match the IUT-T WDM grid which specifies the frequency of the used optical channels according to the value of the optical frequency spacing such as 50, 100, and 150 GHz.

(ii) The line frequency spacing Δf of the designed comb is controlled by the RF frequency f_{RF} and yields $\Delta f = f_{RF}$. Therefore, f_{RF} of 50, 100, and 150 GHz are used to design 50 GHz-, 100 GHz-, and 150 GHz-channel spacing WDM systems, respectively. A CW laser whose frequency matches one of the channel optical frequencies fixed in the grid is used to excite the comb. For example, consider an 8-channel WDM system designed with $\Delta f = 100$ GHz. When the comb is driven by 193.1 THz CW laser, the used eight lines of the comb are 192.8, 192.9, 193.0, 193.1, 193.2, 193.3, 193.4, and 193.5 THz. The corresponding channel numbers are Ch1, Ch2,, Ch7, and Ch8, respectively. The central channel corresponds to the 5th channel whose frequency equals the frequency of the used laser.

(iii) The bandwidth of the modulated comb line (i.e., modulated optical carrier) $B_{mo} \approx (1+r)R_s$ where r is the roll-off parameters of the raised-cosine filter used to shape the optical pulses (symbols) and R_s is the symbol rate. The parameter B_{mo} should be less than channel frequency spacing Δf to ensure negligible overlapping between the spectra of neighboring channels in the WDM optical multiplexer and demultiplexer. In this work, 50, 100, and 150 GHz channel spacing comb-based WDM systems are designed with $R_s = 40, 80, \text{ and } 120$ GSps, respectively. To keep $B_{mo} < \Delta f$, the parameter r should be less than $(B_{mo}/R_s) - 1 = 0.2$

Comb Line Spacing Δf (GHz)	Symbol Rate R_s (GSps)	Number of Channels N_{ch}	Bite Rate per Channel R_b (Gbps)	Total Threshold Bitrate (Tbps)
50	40	8	320	2.56
		16		5.12
		32		10.24
		72		23.64
100	80	8	640	5.12
		16		10.2
		32		20.48
		72		46.08
150	120	8	960	7.65
		16		15.36
		32		30.72
		72		69.12

(iv) The designed basic comb offers 25 and 31 lines with 0.5- and 1 dB-flatness spectra, respectively. Therefore, the design of the comb-based WDM systems is limited in those work with $N_{ch} = 8, 16, \text{ and } 32$. Extended N_{ch} to 72 is obtained when the three-output port 72-line comb is used.

(v) For DP M-QAM signaling, the bit rate per WDM channel R_b is related to the symbol rate R_s by

$$R_b = 2R_s \text{Log}_2 M \quad (13)$$

where Log_2M is the number of bits carried by each symbol. The parameter R_b is also called bit rate per λ . The total bit rate $(R_b)_{\text{tot}}$ carried by the WDM system is equal to $N_{\text{ch}} R_b$ where N_{ch} is the number of the WDM channels. Table II lists the values of bit rate per channel for different values of comb lines spacing assuming $R_s/\Delta f = 0.8$ and DP 16-QAM signaling. The corresponding total transmission bit rate for a different number of multiplexed optical lines N_{ch} is also given.

Table II Bite rate per channel and total transmission bit rate corresponding to different values of Δf and N_{ch} . DP 16QAM signalling with $R_s = 0.8 \Delta f$ is assumed

vi) The group-velocity dispersion (GVD) of a SSF is wavelength dependant and therefore, a DSP is used for each channel receiver to compensate the effect of fiber dispersion at that channel wavelength. The DSP uses given values of fiber GVD parameter D and its slope $S = dD/d\lambda$ at a reference wavelength λ_0 to calculate GVD parameters at the channel wavelength λ_i according to

$$D(\lambda_i) = D(\lambda_0) + (\lambda_i - \lambda_0) S \quad (14)$$

In fact, a DP DSP is adopted in the channel receiver used in this work. This DSP tries to compensate the fiber GVD for both Y-and -X- components transmission using the fiber polarization-mode dispersion as an input parameter. Further, this DSP is also used to reduce the effect of nonlinear fiber optics due to Kerr effect.

(vii) The BERs of all the received WDM channels are kept under observation during transmission. The maximum reaches L_{max} is estimated as the maximum length of the transmission link that yields BER less than a threshold value BER_{th} for all the WDM channels. In this work, a threshold BER of 3.8×10^{-3} is used which corresponds to 7% hard-decision forward error correcting (HD-FEC) code.

The BER is usually used as an important parameter in characterizing the performance of data transmission in communication systems. The BER is calculated as the ratio of the number of bits received with error over the number of total received bits. Since the WDM system uses a DP-channel receiver, the BER of each received channel is computed as the average value of the BERs of the two receiver polarization components.

Simulation Result of 8-, 16-, and 32-Channel Comb-based WDM System

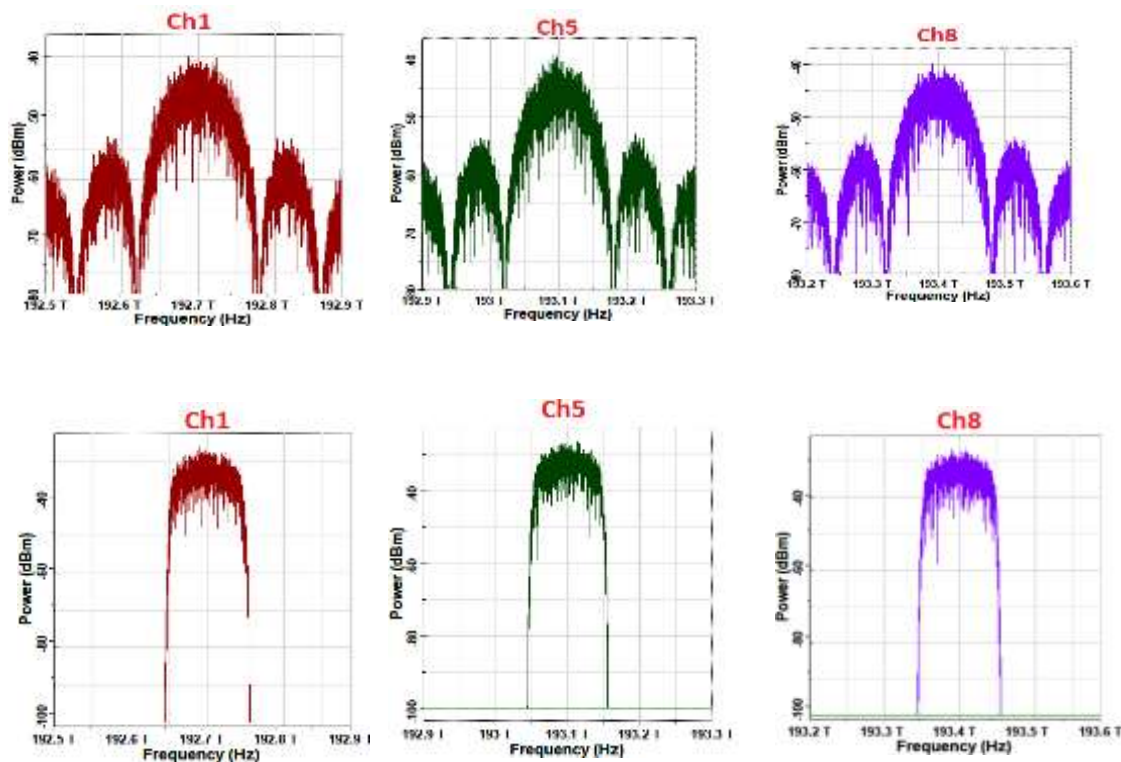
This part presents the simulation results to characterize the transmission performance of 8-, 16-, and 32-channel C-band coherent WDM systems using the OFCG proposed in the previous section. Results are obtained for different values of comb line spacing Δf (50, 100, and 150 GHz) assuming symbol rate R_s of 40, 80, and 120 GSps, respectively. The corresponding bit rate per channel $R_b = 320, 640, \text{ and } 960$ Gbps assuming DP 16-QAM modulation format. Unless otherwise stated, the system main components and related parameters values used in the simulation are listed in Table III

Table III Main system components and related parameters values used in the simulation.

Subsystem	Components	Parameters	Value
Optical Frequency Comb Generator	CW Laser	Frequency	193.1 THz
		Power	20 dBm
	Mach-Zehnder Modulator 1	Bias	$V\pi/2 (= 1.75V)$
		Modulation Index	1
		Losses	0 dB
	Mach-Zehnder Modulator 2	Bias	$V\pi (= 3.5v)$
		Modulation Index	0
		Losses	0 dB
	Electroporation Modulator	Modulation Index	0.5
		Chirp	125
Losses		0 dBm	
RF Oscillator	Frequency Comb Line Spacing Δf	50, 100, and 150 GHz	
Channel Transmitter	Modulation Format	DP 16-QAMm	
	Symbol Rate	40, 80 and 120 GSps	

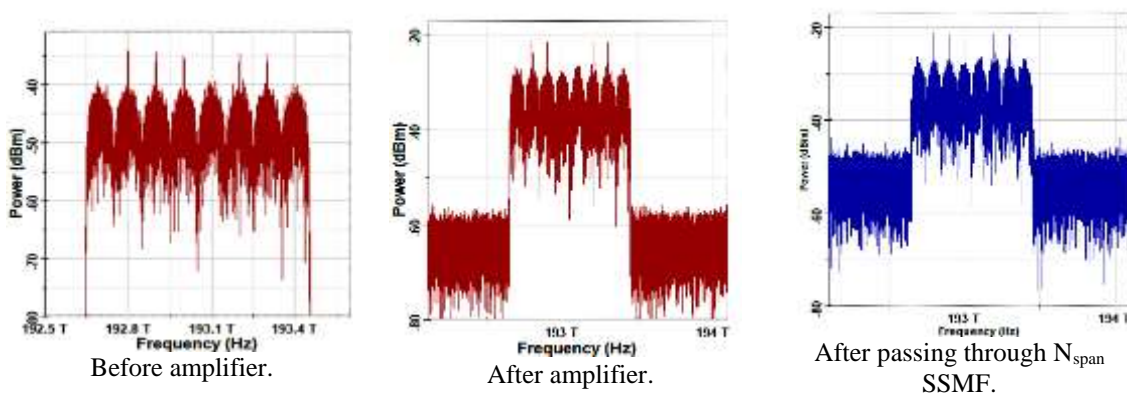
WDM Transmitter		Number of Channels	8, 16, and 32
	Booster Optical Amplifier	Gain	14 dB
		Noise Figure	4 dBm
Transmission Link	(SSMF) Span	Length	80 km
		Group Velocity Desperation To @1550 nm	16.75 ps/(nm.km)
		Dispersion Slope At @1550 nm	0.075 ps/nm²/km
	Optical Amplifier	Gain	16 dB
		Noise Figure	4 dB
WDM Receiver	Channel Receiver	Type	Coherent-Detection DP-16-QAM
		Optical Demodulator	DP-IQ Demodulator
		Photodiode	PIN of 1 A/W Responsivity @ 1550nm and 10 nA Dark Current
		Digital Signal Processor	DP 16-QAM DSP With 1550nm
OFCG Demultiplexer		Filter Bandwidth	5 GHz
		Filter Order	10
		Filter Type	Gaussian
		Losses	0 dB
Transmitter Demultiplexer and Receiver Demultiplexer		Filter Bandwidth	0.9 Δf
		Filter Type	Gaussian
		Filter Order	10
		Losses	0 dB

Figure 14 illustrates the spectra of the signals at different points of the 8-channel DP 16-QAM WDM system designed with a 100-GHz line spacing comb. The spectra and received constellation diagrams of three channels, namely the first channel (Ch1) central channel (Ch5), and last channel (Ch8), are kept under observation. The transmission distance is set to 11 spans which correspond to the maximum reach in this case. A symbol rate R_s of 80 GSps is considered which yields 640 Gbps per channel and 5.12 Tbps total data transmission. The DSP parameters of each channel are tuned carefully to compensate the effect of fiber impairments as seen by comparing the channel constellation diagrams before and after DSP as depicted in Figure 14 e. Note that the bandwidth of each of the channel optical modulated signals is approximately equal to 80 GHz corresponding to R_s .



(a) Spectra of Ch1, Ch5 and Ch8 at the transmitter side.

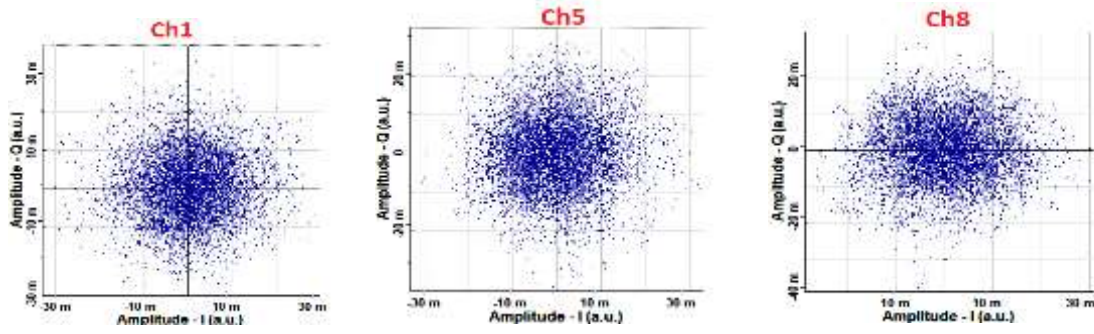
Fig 14: Spectra of signals at different points of the 8-channel DP 16-QAM WDM system designed with 100-GHz line spacing comb.



(b) Multiplexed signal.

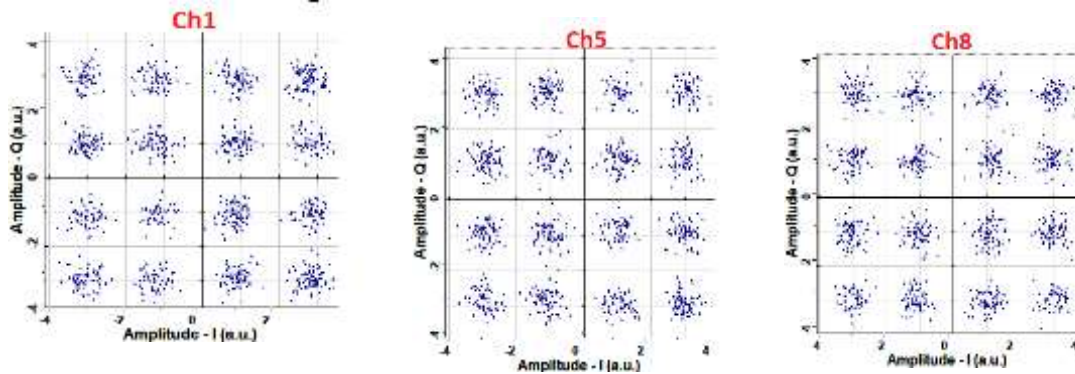
(c) Spectra of Ch1, Ch5, and Ch8 at the receiver side.

(d)



Constellation diagrams before DSP.

Fig 14: (Continued).



(e) Constellation diagrams after DSP.

Figure 14: (Continued).

Figure 15 shows the variation of BER at the receiver side as a function of a number of 80 km-spans for DP 16-QAM WDM system designed with 50 GHz and 100 GHz-line spacing comb. The value of R_s is set to 40 and 80 GSps, respectively. The results in the Figure are presented for three values of a number of WDM channels, namely 8, 16, and 32. The BER of the WDM system is estimated as the maximum BER among the three channels (first, center, and last). The results in this Figure can be used to deduce the maximum reach L_{max} considering $BER_{th} = 3.8 \times 10^{-3}$ where L_{max} is measured by a number of spans when all the channels yield received $BER < BER_{th}$ under the condition that after extra span, one of the channels at least yields $BER > BER_{th}$.

The dependence of the maximum reach on the number of WDM multiplexed channels and comb line spacing Δf is listed in Table IV. Recall that the symbol rate $R_s = 0.8 \Delta f$ is used in this simulation. The table also includes the bit rate-distance product (BDP) for each case which can be used as an additional performance measure. The parameter BDP is calculated using the following equation assuming DP M-QAM modulation format

$$\begin{aligned} \text{BDP} &= \text{Total transmission bit rate} \times \text{Maximum reach} \\ &= 2N_{ch} R_s (\text{Log}_2 M) L_{max} \end{aligned} \quad (15a)$$

$$= 1.6 N_{ch} \Delta f (\text{Log}_2 M) L_{max} \quad (15b)$$

Note that L_{max} is also a function of N_{ch} , R_s , and M . investigating the results reveal the following findings.

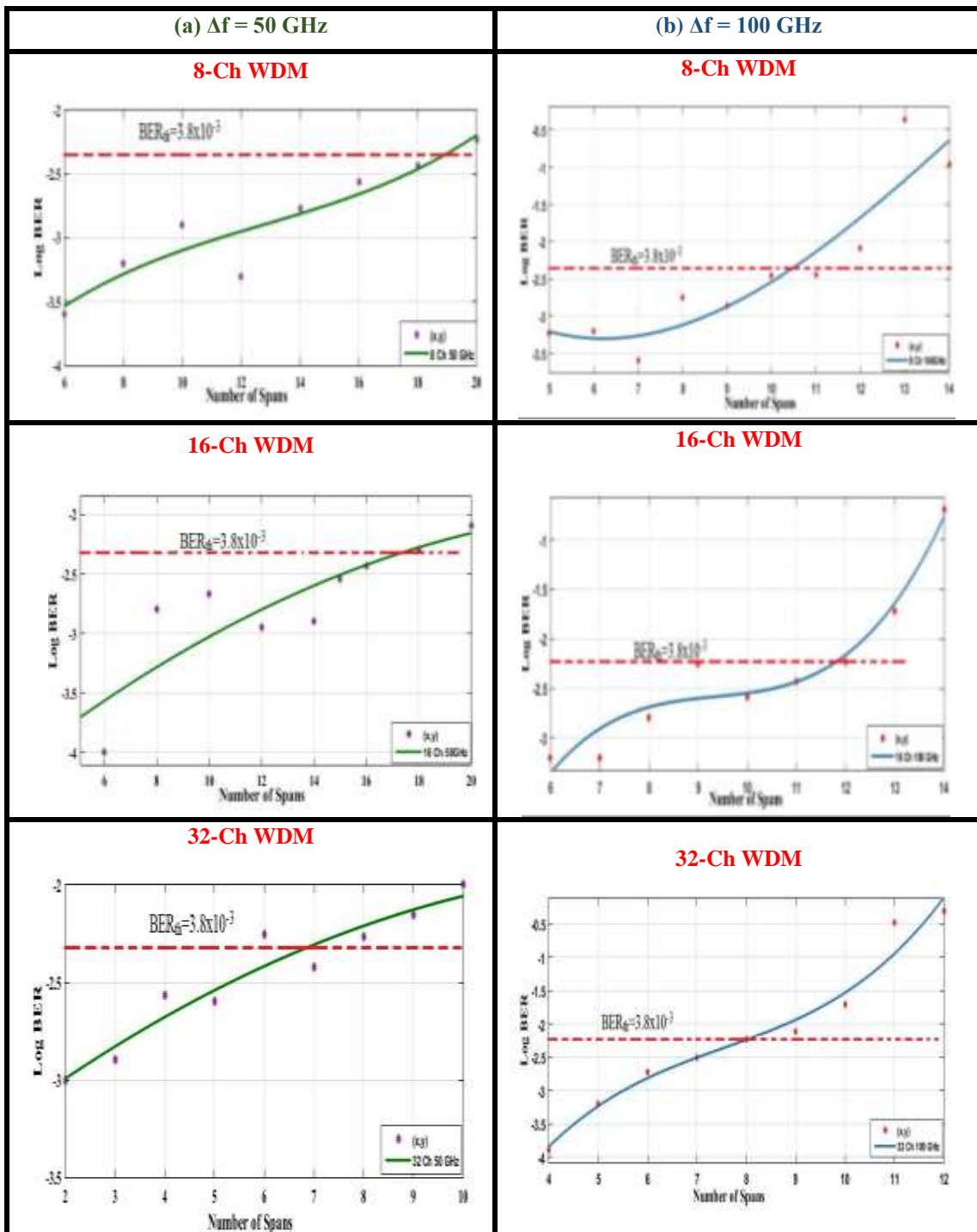


Fig 15: BER at the receiver side as a function of number of 80km-spans for DP-16-QAM WDM system. The symbol rate is set to $0.8 \Delta f$.

Table IV Dependence of maximum reach and bit rate-distance product BPD on the number of multiplexed channel and comb line spacing Δf for DP 16-QAM Comb WDM system operating with symbol rate = $0.8 \Delta f$.

Comb Line Spacing Δf (GHz)	Number of Multiplexed Channels N_{ch}	Maximum Reach L_{max} (80km-span)	Bit rate-Distance Product (Tbps.km)
50	8	18	3686.4
	16	16	6553.6
	32	7	5734.4
100	8	11	4505.6
	16	11	9011.2
	32	7	11468.8
150	8	8	4915.2
	16	7	8601.6
	32	7	17203.2

Transmission performance of 72-Line Comb-Based WDM System

The 72-line OFCG proposed in the previous section is used here to design a 72-channel comb-based WDM system. The comb offers 72 spectral lines of 100 GHz spacing covering the whole C band. Recall that this OFCG uses inherent three 24-line combs covering three subbands: SB1 from 190.1 to 192.4 THz, SB2 from 192.5 to 194.8 THz, and SB3 from 194.9 to 197.2 THz, respectively. Assuming DP 16-QAM modulation format and 80 GSps ($= 0.8 \times \Delta f$) symbol rate, the total transmission bit rate $(R_b)_{tot} = 2 \times 80 (\log_2 16) \times 72 = 46.08$ Tbps. The transmission performance of this WDM system is simulated using the parameters values given in Table III.

Figure 16 shows the configuration of the coherent 72-channel WDM system under investigation when two 72-line OFCGs are used, one at the transmitter side and the other at the receiver side. In this figure, the optical and electrical interconnect are distinguished by red and blue colors, respectively. Also, the optical interconnector is presented by either a thin or a thick line to denote a single-lane or 24-lane link, respectively. The 24-lane link consists of 24 parallel single-lane interconnect. Few remarks related to Figure 16 are given in the following

- (i) The OFCG has three ports each one of them provides 24-line spectral comb characteristics. The output of each port is applied to a 1:24 demultiplexer to yield the 24 optical carriers for the corresponding WDM subband.
- (ii) A band of 72 optical modulators (optical receivers) can be used to replace the three banks of 24-subband optical modulators (optical receivers).
- (iii) The booster and in-line optical amplifiers can be implemented using EDFA system. Each type of the optical amplifier has a wide amplifications bandwidth in C band (≈ 10 THz) and can be amplifying the 72 100 GHz-spacing WDM signal (72 THz).

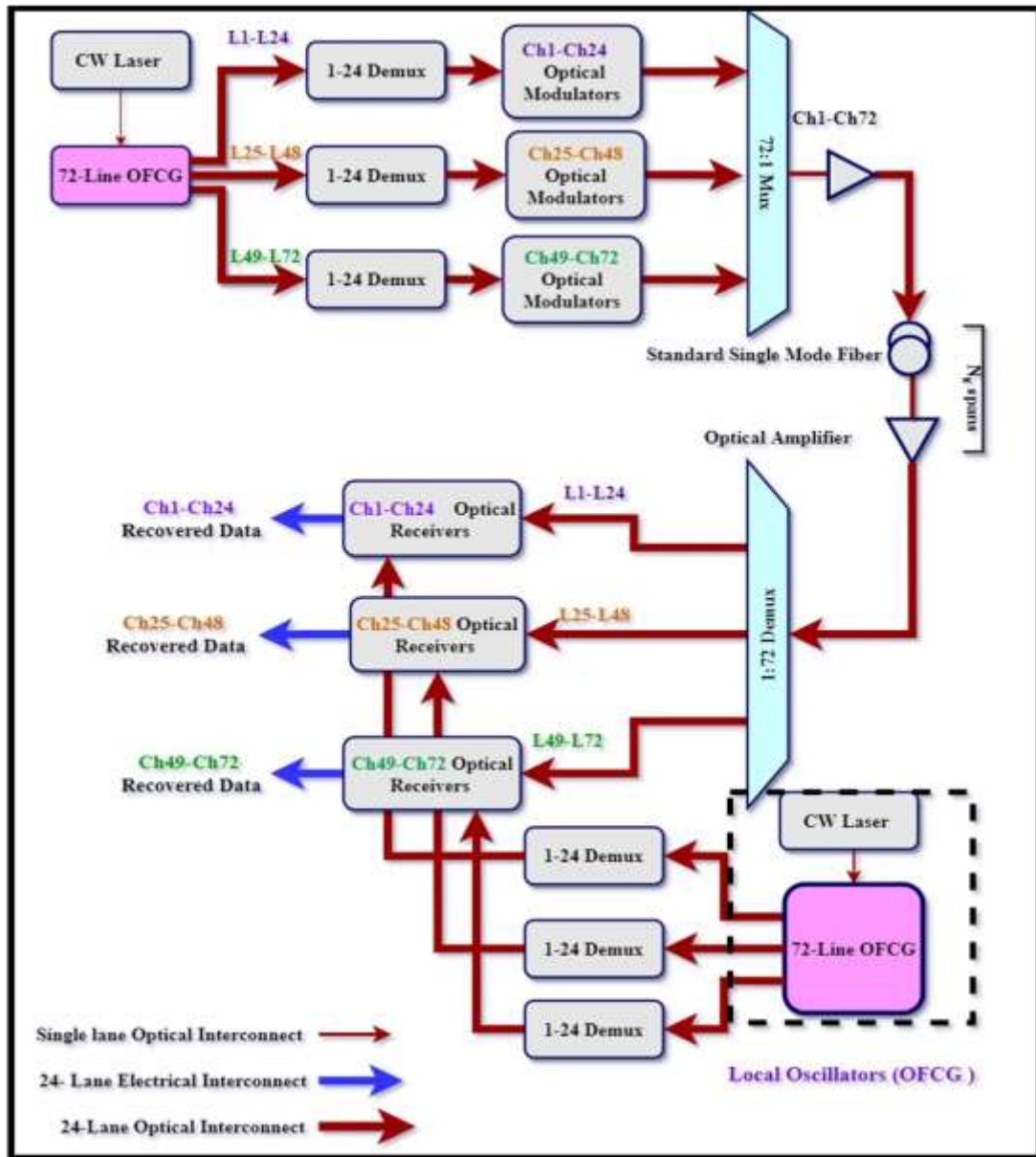
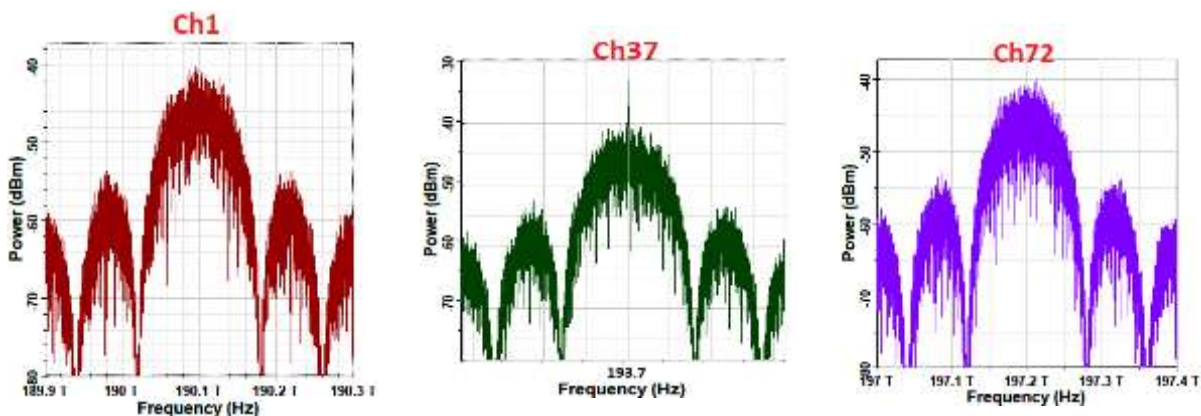
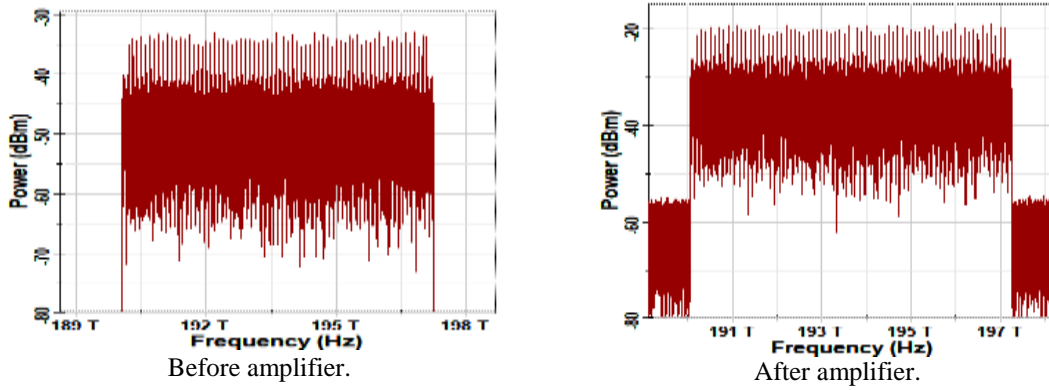


Fig 16: Block Diagram of the coherent 72-channel comb-based WDM system.

The system in Figure 16 is simulated assuming a symbol rate of 80 GSps and DP 16-QAM signaling. The results are given in Figure 17 which shows the spectra of the three subband WDM signals and total WDM signal at the transmitter side along with the received WDM signal at the fiber end. Further, the figure contains the received constellation diagrams of three channels (Ch1, Ch37, and Ch72) after 5 spans (400 km) of transmission which corresponds to maximum reach in this case.

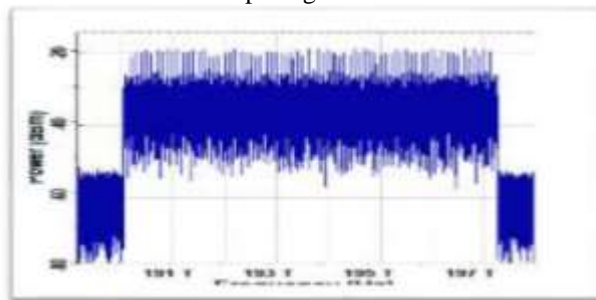


(a) The spectra of Ch1, Ch37, and Ch72 at the transmitter side.

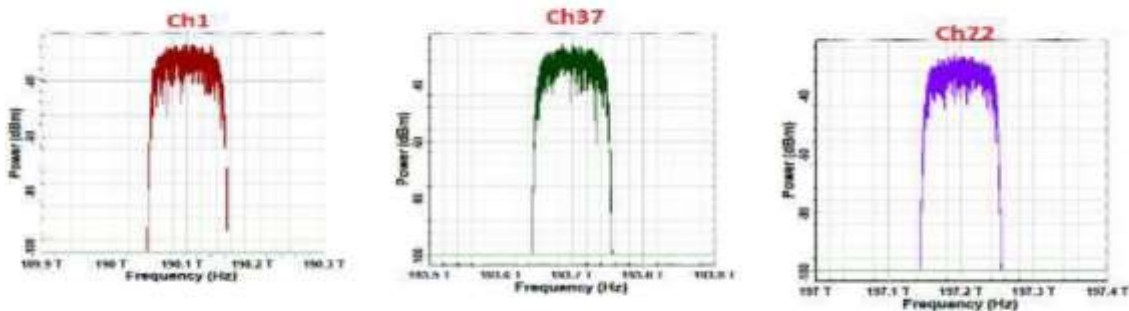


(b) Multiplexed signal.

Fig 17: Spectra of the signal at different points of 72-channel DP 16-QAM WDM system designed with 100-GHz line spacing comb.

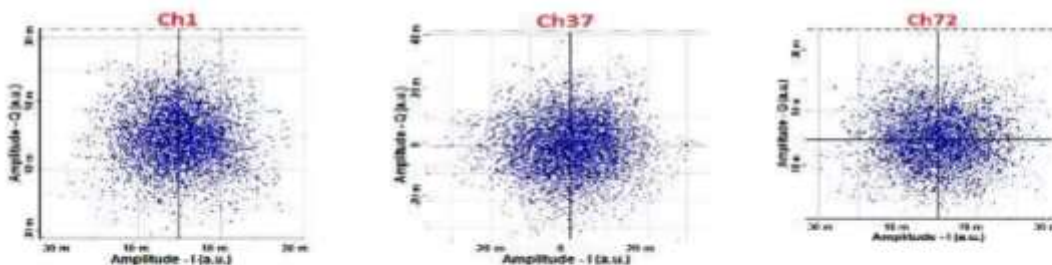


(c) Multiplexed signal after passing through N_{span} SSFM



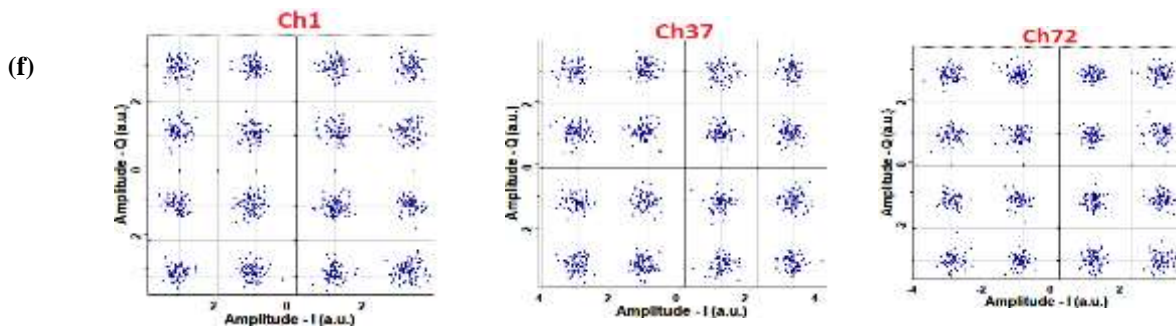
Spectra of Ch1, Ch37, and Ch72 at the receiver side.

(d)



(e) Constellation diagrams before DSP.

Fig 17: (Continued).



Constellation diagrams after DSP.

Fig 17: (Continued).

The variation of received BER with a number of transmitting spans is shown in Figure 18. The results indicate that $L = 5$ spans and here the corresponding BDP = 18432 THz.km.

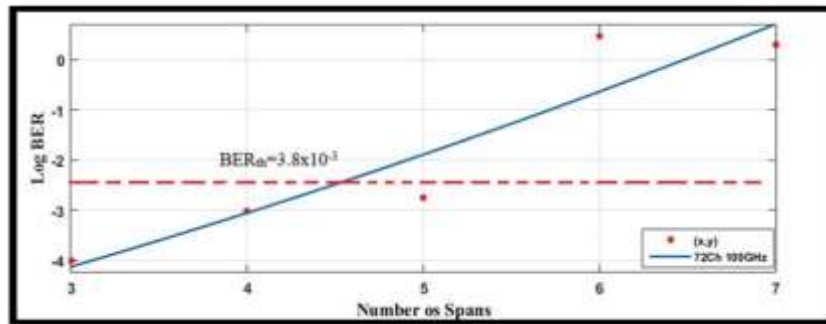


Fig 18: BER at the receiver side as a function of a number of 80km-span for 72-channel comb-based WDM system with $\Delta f = 100\text{GHz}$ $R_s = 0.8 \Delta f$, and DP 16-QAM signalling.

VI. CONCLUSIONS

An UWB OFCG has been designed using two parallel Mach-Zehnder modulators MZMs cascaded with EOM. The proposed comb has been used as a basic unit to develop a higher-spectrum comb. The designed comb configurations have been used in DP 16-QAM coherent WDM systems operating with 8, 16, and 32 channels and with 40, 80, and 120 Gbps symbol rates. The transmission performance of the designed comb-based WDM systems has been simulated using Optisystem software ver.15. The main conclusions drawn from this study are

- (i) The proposed comb unit can offer 25 and 37 lines within 0.5- and 1- dB-flatness spectra, respectively. The number of lines is independent on line frequency spacing Δf which is controlled by the frequency of the RF oscillator.
- (ii) The proposed comb unit is characterized by a 1dB-flatness spectrum bandwidth of 1.55, 3.1, and 4.65 THz when it is designed with $\Delta f = 50, 100,$ and 150 GHz, respectively.
- (iii) A three-port 72-line comb configuration has been developed from the proposed comb unit to support 72-channel extended C-band operation with 100 GHz channel spacing.
- (iv) The comb line frequency spacing Δf can be tuned easily to support DP 16-QAM WDM system operating with 320, 640, and 960 Gbps bit rate when $\Delta f = 50, 100,$ and 150 GHz respectively.
- (v) When Δf is fixed, increasing the number of multiplexed channels N_{ch} may lead to a decrease in the number of transmission spans N_{span} link. The length of the transmission link is reduced to 89 % and 39 % when the 8 multiplexed channels are replaced by 16 and 32 channels respectively, and assuming $\Delta f = 50$ GHz these values are to be compared with (100% and 64%) and (88% and 88%) when $\Delta f = 100\text{GHz}$ and 150 GHz respectively.
- (vi) The highest value of BDP is 17203 Tpbs.km which is obtained when the system is designed with $N_{ch} = 32$ and $\Delta f = 150$ GHz. This system can offer 30.72 Tpbs data rate over 7-span SSMF.

REFERENCES

- [1] D. Hastbacka, J. Halame, L. barana, h. Hoikka, H. Pettinen, M. Larrañaga, M. Björkbom, H. Mesiä, A. Jaatinen. and M. Elo, "Dynamic edge and cloud service integration for industrial IOT and production monitoring applications of industrial cyber-physical systems," *IEEE Transactions on Industrial Informatics*, vol. 18, no. 1, pp. 498–508, Jan. 2022, doi: 10.1109/TII.2021.3071509.

- [2] T. Pfeiffer, P. Dom, S. Bidkar, F. Fredricx, K. Christodouloupoulos, and R. Bonk, "PON going beyond FTTH," *Journal of Optical Communications and Networking*, vol. 14, no. 1, pp. A31–A40, Jan. 2022, doi: 10.1364/JOCN.439241.
- [3] P. Wang, W. Xiong, Z. Huang, Y. He, J. Liu, J. Xiao, Y. Li, D. Fan, and S. Chen, "Diffraction deep neural network for optical orbital angular momentum multiplexing and demultiplexing," *IEEE Journal of Selected Topics in Quantum Electronics*, vol. 28, no. 4, Jul. 2022, doi: 10.1109/JSTQE.2021.3077907.
- [4] A. Matsushita, M. Nakamura, S. Yamamoto, F. Hamaoka, and Y. Kisaka, "41-Tbps C-band WDM transmission with 10-bps/hz spectral efficiency using 1-tbps/ λ signals," *IEEE Journal of Lightwave Technology*, vol. 38, no. 11, pp. 2905–2911, Jun. 2020, doi: 10.1109/JLT.2020.2986083.
- [5] C. Manso, R. Munoz, N. Yoshikane, R. Vilata, R. Martinez, T. Tsuritani, and I. Morita "TAPI-enabled SDN control for partially disaggregated multi-domain (OLS) and multi-layer (WDM over SDM) optical networks," *Journal of Optical Communications and Networking*, vol. 13, no. 1, pp. A21–A33, Jan. 2021, doi: 10.1364/JOCN.402187.
- [6] B. C. Chatterjee and E. Oki, *Elastic optical networks fundamentals, design, control, and management*, CRC Press, 2020.
- [7] M. Mazur, J. Schroder, A. Lorences-Riesgo, T. Yoshida, M. Karlsson, and P. A. Andrekson, "12 b/s/Hz spectral efficiency over the C-band based on comb-based superchannels," *IEEE Journal of Lightwave Technology*, vol. 37, no. 2, pp. 411–417, Jan. 2019, doi: 10.1109/JLT.2018.2880249.
- [8] D. J. Blumenthal, H. Ballani, O. Behuin, E. Bowers, P. Costa, D. Ilenoski, A. Morton, and P. Papp, T. Rakich "Frequency-stabilized links for coherent WDM fiber interconnects in the datacenter," *IEEE Journal of Lightwave Technology*, vol. 38, no. 13, pp. 3376–3386, Jul. 2020, doi: 10.1109/JLT.2020.2985275.
- [9] V. Torres-Company, J. Schroder, A. Fulop, M. Mazur, L. Lundberg, B. Helgason, M. Karlsson, and P. Andrekson "Laser frequency combs for coherent optical communications," *IEEE Journal of Lightwave Technology*, vol. 37, no. 7, pp. 1663–1670, Apr. 2019, doi: 10.1109/JLT.2019.2894170.
- [10] M. Mazur, A. Lorences-Riesgo, J. Schroder, P. A. Andrekson, and M. Karlsson, "10 Tb/s PM-64QAM Self-Homodyne Comb-Based Superchannel Transmission with 4% Shared Pilot Tone Overhead," *IEEE Journal of Lightwave Technology*, vol. 36, no. 16, pp. 3176–3184, Aug. 2018, doi: 10.1109/JLT.2018.2820166.
- [11] S. Spolitis, R. Murnieks, L. Skladova, T. Salgals, V. A. Andrianov, P. M. Marisova, G. Leuchs, A. E. Anashkina, and V. Bobrovs "IM/DD WDM-PON communication system based on optical frequency comb generated in silica whispering gallery mode resonator," *IEEE Access*, vol. 9, pp. 66335–66345, 2021, doi: 10.1109/ACCESS.2021.3076411.
- [12] M. Mazur, G. Suh, A. Fulop, J. Schroder, V. Torres-Company, M. Karlsson, K. Vahala, and P. Andrekson, "High spectral efficiency coherent superchannel transmission with soliton microcombs," *IEEE Journal of Lightwave Technology*, vol. 39, no. 13, pp. 4367–4373, Jul. 2021, doi: 10.1109/JLT.2021.3073567.
- [13] D. Kong, E. da Silva, Y. Sasaki, K. Aikawa, F. Da Ros, M. Galili, T. Morioka, H. Hu, and L. Oxenloewe, "909.5 Tbit/s Dense SDM and WDM transmission based on a single source optical frequency comb and Kramers-Kronig Detection," *IEEE Journal of Selected Topics in Quantum Electronics*, vol. 27, no. 2, pp. 1–8, Sep. 2020, doi: 10.1109/jstqe.2020.3024004.
- [14] A. Parriaux, K. Hammani, and G. Millot, "Electro-optic frequency combs," *Advances in optics and photonics*, vol. 12, no. 1, p. 223-288, Mar. 2020, doi: 10.1364/aop.382052.
- [15] H. Hu and L. K. Oxenloewe, "Chip-based optical frequency combs for high-capacity optical communications," *Nanophotonics*, vol. 10, no. 5, De Gruyter Open Ltd, pp. 1367–1385, Mar. 01, 2021, doi: 10.1515/nanoph-2020-0561.
- [16] A. Fülöp, M. Mazur, T. A. Eriksson, P. A. Andrekson, V. Torres-Company, P. Wang, Y. Xuan, D. E. Leaird, M. Qi, and A. M. Weiner "Long-haul coherent transmission using a silicon nitride microresonator-based frequency comb as WDM source," Conf. on Lasers and Electro-Optics Optical, Society of America, San Jose, California United States, 5–10 June 2016.
- [17] J. Lin, L. Wang, M. Lyu, A. Pai, X. Zhang, S. LaRochelle, and L. A. Rusch "Demonstration and evaluation of an optimized RFS comb for terabit flexible optical networks," *IEEE Journal of Optical Communications and Networking*, vol. 9, no. 9, pp. 739–746, Sep. 2017, doi: 10.1364/JOCN.9.000739.
- [18] P. Marin-Palomo, J. N. Kemal, P. Trocha, S. Wolf, K. Mergem, F. Lelarge, A. Ramdane, W. Freude, S. Randel, and Christian Koos, "Comb-based WDM transmission at 10 Tbit/s using a DC-driven quantum-dash mode-locked laser diode," *Optics Express*, vol. 27, no. 22, pp. 31110–31129, Oct. 2019, doi: 10.1364/oe.27.031110.
- [19] B. Corcoran, M. Tan, X. Xu, A. Boes, J. Wu, T. G. Nguyen, S. T. Chu, B. E. Little, R. Morandotti, A. Mitchell and D. J. Moss "Ultra-dense optical data transmission over standard fibre with a single chip source," *Nature Communications*, vol. 11, no. 1, Dec. 2020, doi: 10.1038/s41467-020-16265-x.
- [20] C. Prayonyong, A. Boes, X. Xu, M. Tan, S. T. Chu, B. E. Little, R. Morandotti, A. Mitchell, D. J. Moss, and B. Corcoran, "Frequency comb distillation for optical superchannel transmission," *IEEE Journal of Lightwave Technology*, vol. 39, no. 23, pp. 7383–7392, Dec. 2021, doi: 10.1109/JLT.2021.3116614.
- [21] J. Lin, H. Sephrian, Y. Xu, L. A. Rusch, and W. Shi, "Frequency comb generation using a CMOS compatible SiP DD-MZM for flexible networks," *IEEE Photonics Technology Letters*, vol. 30, no. 17, pp. 1495–1498, Sep. 2018, doi: 10.1109/LPT.2018.2856767.
- [22] Z. Wang, M. Ma, H. Sun, M. Khalil, R. Adams, K. Yim, X. Jin, L. R. Chen "Optical frequency comb generation using CMOS compatible cascaded mach-zehnder modulators," *IEEE Journal of Quantum Electronics*, vol. 55, no. 6, Dec. 2019, doi: 10.1109/JQE.2019.2948152.
- [23] E. A. Anashkina and A. v. Andrianov, "Kerr-Raman Optical Frequency Combs in Silica Microsphere Pumped near Zero Dispersion Wavelength," *IEEE Access*, vol. 9, pp. 6729–6734, 2021, doi: 10.1109/ACCESS.2021.3049183.
- [24] B. Buscaino, M. Zhang, M. Lončar, and J. M. Kahn, "Design of efficient resonator-enhanced electro-optic frequency comb generators," *IEEE Journal of Lightwave Technology*, vol. 38, no. 6, pp. 1400–1413, Mar. 2020, doi: 10.1109/JLT.2020.2973884.

- [25] S. Ullah, R. Ullah, Q. Zhang, H. Khalid, K. A. Memon, A. Khan, F. Tian, and X. Xia, "Ultra-wide and flattened optical frequency comb generation based on cascaded phase modulator and LiNbO₃-MZM offering terahertz bandwidth," *IEEE Access*, vol. 8, pp. 76692–76699, 2020, doi: 10.1109/ACCESS.2020.2989678.
- [26] H. Francis, X. Zhang, S. Chen, J. Yu, K. Che, M. Hopkinson, and C. Jin, "Optical Frequency Comb Generation via Cascaded Intensity and Phase Photonic Crystal Modulators," *IEEE Journal of Selected Topics in Quantum Electronics*, vol. 27, no. 2, Mar. 2021, doi: 10.1109/JSTQE.2020.3041936.
- [27] L. Deniel, E. Weckenmann, D. P. Galacho, C. Lafforgue, S. Monfray, C. Alonso-Ramos, L. Bramerie, F. Boeuf, L. Viven, and D. Marris-Morini, "Silicon photonics phase and intensity modulators for flat frequency comb generation," *Photonics Research*, vol. 9, no. 10, pp. 2068-2076, Oct. 2021, doi: 10.1364/prj.431282.
- [28] H. J. Weber, F. Harris, and G. B. Arfken "Essential Mathematical Methods for Physicist and Engineers" Academic Press 2004.
- [29] Y. Cheng, J. Yan, S. Zhao, "Self-oscillating parametric optical frequency comb generation using an electroabsorption modulated laser-based optoelectronic oscillator," *IEEE Photonics Journal*, vol. 11, no. 4, Aug. 2019, doi: 10.1109/JPHOT.2019.292881